

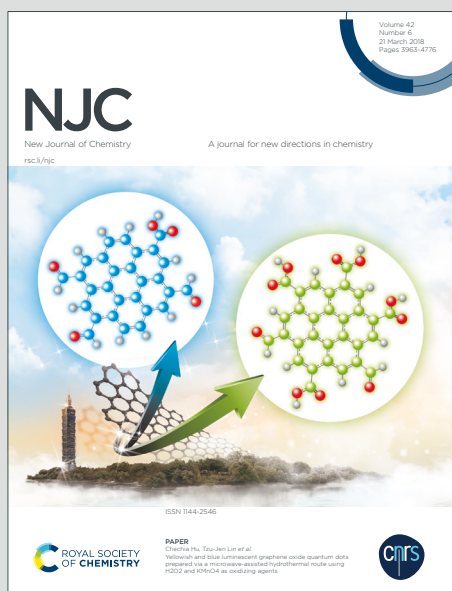
NJC

New Journal of Chemistry

Accepted Manuscript

A journal for new directions in chemistry

This article can be cited before page numbers have been issued, to do this please use: V. Varmuzova, I. Cisarova and P. Štřprika, *New J. Chem.*, 2026, DOI: 10.1039/D6NJ01330A.



This is an Accepted Manuscript, which has been through the Royal Society of Chemistry peer review process and has been accepted for publication.

Accepted Manuscripts are published online shortly after acceptance, before technical editing, formatting and proof reading. Using this free service, authors can make their results available to the community, in citable form, before we publish the edited article. We will replace this Accepted Manuscript with the edited and formatted Advance Article as soon as it is available.

You can find more information about Accepted Manuscripts in the [Information for Authors](#).

Please note that technical editing may introduce minor changes to the text and/or graphics, which may alter content. The journal's standard [Terms & Conditions](#) and the [Ethical guidelines](#) still apply. In no event shall the Royal Society of Chemistry be held responsible for any errors or omissions in this Accepted Manuscript or any consequences arising from the use of any information it contains.

ARTICLE

Synthesis, coordination and catalytic application of hybrid phosphinoferrocene ligands bearing imidazole N-donor groups

Věra Varmužová, Ivana Císařová and Petr Štěpnička*

Received 00th January 2026,
Accepted 00th January 2026

DOI: 10.1039/x0xx00000x

Hybrid P,N-donors are versatile ligands in coordination chemistry and catalysis, capable of forming hemilabile coordination bonds. This article describes the preparation of three structurally related hybrid phosphinoferrocene donors bearing 1-methyl-1*H*-imidazol-2-yl pendants attached *via* CH(OH), C=O, and CH₂ linkers at position 1' of the ferrocene unit, Ph₂PfcYIm^{Me} (fc = ferrocene-1,1'-diyl, Im^{Me} = 1-methyl-1*H*-imidazol-2-yl, and Y = the linker). Coordination behaviour of these compounds towards soft Pd(II) strongly depends on the nature of the linker: the flexible nonconjugated linkers (CH(OH) and CH₂) enable P,N-chelate coordination, whereas a similar coordination of the ketone appears to be hindered by the linker's tendency to remain conjugated and by its ability to decrease electron density at the imidazole unit. As a result, complexes of types [PdCl₂(L-κ²P,N)] and [Pd(L-κ²P,N)₂][BF₄]₂ could be obtained from the former compounds, whereas the C=O-bridged ligand afforded the bis-phosphine complex [PdCl₂(L-κP)₂] as the only isolable product. The chelate complexes [PdCl₂(Ph₂PfcCH(X)Im^{Me}-κ²P,N)] (X = H and OH) were evaluated in Pd-catalysed Suzuki–Miyaura cross-coupling of 2-bromopyridine with 4-tolylboronic acid, and their catalytic performance was compared with the related compounds, including the widely studied complex [PdCl₂(dppf-κ²P,P')] (dppf = 1,1'-bis(diphenylphosphino)ferrocene).

Introduction

Introducing additional, chemically distinct donor groups into the molecules of phosphine donors¹ increases the coordination diversity of the resulting hybrid ligands. Of particular importance is the potential hemilabile coordination behaviour of these compounds towards soft metal ions, which positively affects the catalytic properties of the resulting complexes.^{1,2} Among the ligand classes reported to date, P,N-hybrid ligands stand out due to their versatility, resulting from the nearly unlimited variation of the phosphine and the N-donor groups.³

Recently,⁴ we reported a series of hybrid and flexible phosphinoferrocene ligands⁵ bearing thiophene and thiazole groups separated from the ferrocene unit by a methylene bridge (compounds **A–C** in Figure 1).⁶ Among these compounds, only thiazole derivative **C** formed an isolable P,N-chelate Pd(II) complex [PdCl₂(**C**-κ²P,N)], which exhibited good catalytic activity in Suzuki–Miyaura-type cross-coupling reactions. To continue this research, we now focus on similar compounds featuring N-methylimidazole pendants (Figure 1). Particular attention is given to the role of the bridging moiety that endows these ligands with additional flexibility and thus affects their coordination behaviour.⁶ Owing to the synthetic approach applied, the linkers include the polar CH(OH) moiety (**1**), the conjugated C=O function (**2**), and the “innocent” CH₂ spacer (**3**). Notably, compounds related to **3** bearing a (benz)imidazole moiety bonded *via* a nitrogen atom have been studied as

precursors to attractive P,C-chelating imidazole-2-ylidene complexes.⁷ A similar coordination mode is not available for **3**.

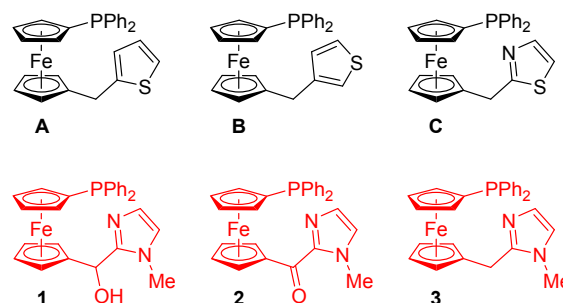


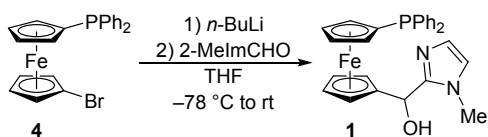
Figure 1 Phosphinoferrocene ligands with heterocyclic functional pendants separated by a flexible linker (**A–C**: known compounds; **1–3**: currently investigated compounds).

Results and discussion

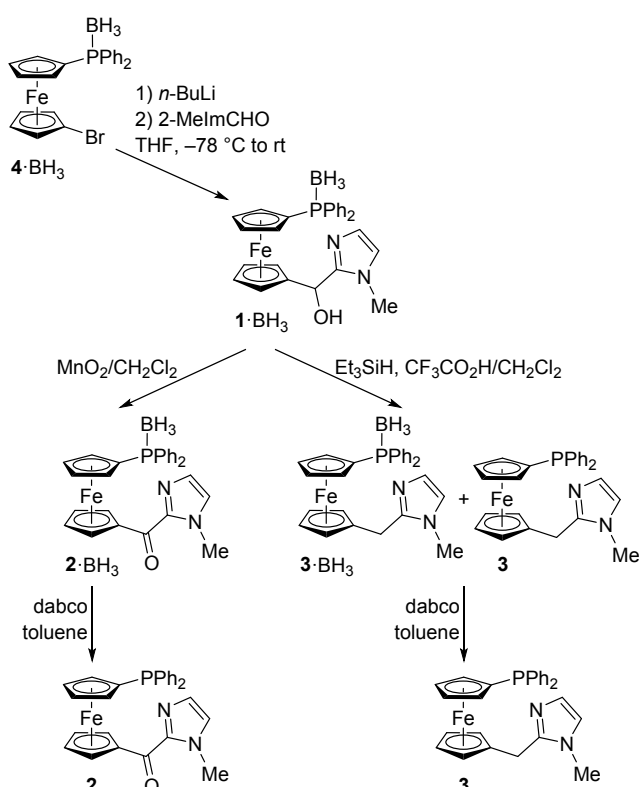
Synthesis and characterisation of hybrid phosphines **1–3**

Compound **1**, possessing a CH(OH) bridging unit, was obtained by lithiation of 1'-(diphenylphosphino)-1-bromoferrocene (**4**)⁸ with *n*-butyllithium and reaction of the nonisolated lithio intermediate with 2-formyl-1-methyl-1*H*-imidazole (Scheme 1). Following aqueous workup and chromatographic purification, it was obtained as an orange solid in 58% yield. Minor amounts (1%) of the corresponding ketone **2** were also isolated.⁹

* Department of Inorganic Chemistry, Faculty of Science, Charles University, Hlavova 2030, 128 00 Prague, Czech Republic; E-mail: stepnic@natur.cuni.cz

Scheme 1 Synthesis of alcohol **1**.

Rational synthesis of ketone **2** (Scheme 2) involved borane-protected intermediates¹⁰ to avoid oxidation of the phosphine moiety during the alcohol-to-ketone conversion. The required intermediate **1**-BH₃ was prepared from borane adduct **4**-BH₃ using the procedure employed for the preparation of **1**. The protected alcohol was subsequently oxidised with MnO₂,¹¹ and the resulting ketone **2**-BH₃ was deprotected with 1,4-diazabicyclo[2.2.2]octane (dabco)^{12,13} to afford **2** in a good overall yield (40% over the three steps).

Scheme 2 Synthesis of hybrid phosphines **2** and **3**.

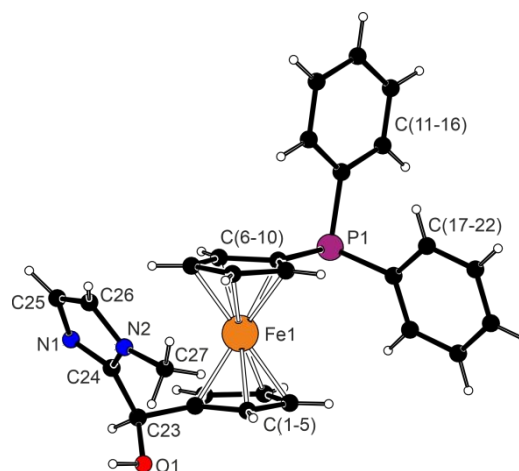
Adduct **1**-BH₃ was also used to prepare the methylene-bridged compound **3** (Scheme 2). In this case, the alcohol was deoxygenated using triethylsilane/trifluoroacetic acid¹⁴ in dichloromethane at room temperature. The reduction required an excess of the reagents to proceed satisfactorily (15 equiv.). No change or poor conversion was observed with 3 or 10 equiv. of Et₃SiH/CF₃CO₂H at room temperature, whereas the reaction with 5 equiv. of Et₃SiH/CF₃CO₂H in refluxing 1,2-dichloroethane produced a complicated mixture containing phosphine oxides. This observation is in accordance with reports demonstrating that the deoxygenation of similar compounds is notoriously difficult.¹⁵ Alternative attempts to reduce **3**-BH₃ using samarium(II) iodide/HMPA and pivalic acid entirely failed,¹⁶

whereas the method reported by Alterman *et al.*¹⁷ using [Mo(CO)₆] and Lawesson's reagent could not be applied due to unwanted thionation of the phosphine group.

Eventually, the reaction of **1**-BH₃ with Et₃SiH/CF₃CO₂H proved reliable but required the excess reagents to be carefully destroyed by aqueous NaHCO₃ during the workup to minimise decomposition. However, the reduction was accompanied by deprotection of the phosphine group, leading to a 65:35 mixture of **3** and **3**-BH₃. The removal of the borane group was completed by treating the mixture with dabco in toluene, affording compound **3** in 30% yield from **1**-BH₃.

All the compounds were characterised using multinuclear NMR spectroscopy, mass spectrometry, and elemental analysis. The characterisation data, particularly the NMR spectra, were consistent with the proposed structures. A distinctive feature was the doubling of the ¹H and ¹³C{¹H} NMR resonances due to the ferrocene and phenyl CH groups in the spectra of **1** and **1**-BH₃, which reflects the diastereotopic nature of these groups resulting from the presence of the stereogenic carbon atom (CHOH). The ³¹P{¹H} NMR signals of the free phosphines were detected at approximately δ_P -17 (in CDCl₃; *cf.* δ_P ≈ -16 for (diphenylphosphino)ferrocene in the same solvent).¹⁸

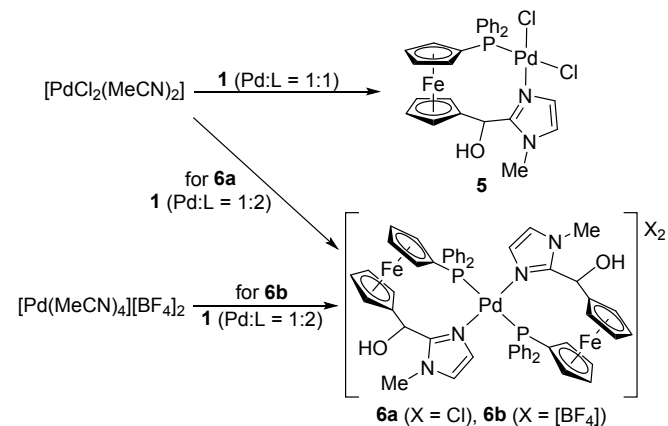
In addition, the structure of **1** was determined by single-crystal X-ray diffraction analysis. The compound is racemic and crystallises in the orthorhombic space group *Pbca* with one molecule in the asymmetric unit (Figure 2). The ferrocene unit has its regular geometry with Fe–C bond lengths in the range of 2.025(3)–2.061(2) Å and negligibly tilted cyclopentadienyl rings (tilt angle: 1.5(2)°).¹⁹ The substituents are diverted from each other, with the C1–Cg1–Cg2–C6 (τ) torsion angle of -162.8(2)° (Cg1 and Cg2 are the centroids of the cyclopentadienyl rings C(1–5) and C(6–10), respectively). The geometry of the substituents is unexceptional in view of the data reported for (diphenylphosphino)ferrocene²⁰ and alcohols ArCH(OH)(Im^{Me}), where Im^{Me} is 1-methyl-1*H*-imidazol-2-yl, and Ar is 1-naphthyl or 2-methoxyphenyl.²¹ In the solid state, the molecules of **1** assemble *via* O1–H1O...N1 hydrogen bonds (O1...N1 = 2.754(3) Å) into chains oriented along the crystallographic *a* axis. These chains are crosslinked by C–H...O interactions (see the SI).

Figure 2 Molecular structure of racemic alcohol **1** (for additional data and the displacement ellipsoid plot, see the SI).

Synthesis of Pd(II) complexes

The coordination behaviour of **1–3** was studied in Pd(II) complexes. Palladium was chosen as a typical soft metal ion with an affinity for both P- and N-donor ligands,²² with the aim of using the complexes in Pd-mediated organic reactions.

The reaction of **1** with an equimolar amount of [PdCl₂(MeCN)₂] as the PdCl₂ source in dichloromethane produced a mixture of two species with similar ³¹P NMR chemical shifts (δ_p 21.3 and 23.9 in CD₂Cl₂). The situation changed after some methanol was added. While the solubility of the products increased with a few drops of this solvent, a larger amount (10-20%) was required to shift the “equilibrium” in favour of one species (δ_p 22.9 in CD₂Cl₂/CD₃OD). One set of NMR signals was also observed in dms_o-d₆, another highly polar solvent (see Experimental and the SI), but the signals appeared shifted, presumably due to solvation effects (δ_p 20.6). The NMR signature indicated simultaneous coordination of the phosphine and imidazole groups, possibly in a chelating manner. This led us to formulate the product as a P,N-chelate complex **5** (Scheme 3), which was indeed confirmed by X-ray crystallography using crystals of **5**·2CHCl₃ obtained by layering the chloroform solution of the complex with hexane (*vide infra*).



Scheme 3 Synthesis of Pd(II) complexes with phosphinoalcohol **1** (the reactions were performed in dichloromethane or dichloromethane-methanol).

A similar reaction employing [PdCl₂(MeCN)₂] and 2 equiv. of alcohol **1** (Scheme 3) initially seemed practically impossible. Analysis using ³¹P{¹H} NMR spectroscopy revealed multiple signal sets attributable to coordinated **1**. Fortunately, crystallisation of the reaction mixture produced several crystals of the cationic bis(chelate) complex **6a** (in solvated form), which was structurally authenticated by single-crystal X-ray diffraction; the expected bis(phosphine) complex [PdCl₂(1-κP)₂] was not isolated, and the reaction mixture slowly degraded.

Next, the reaction was repeated using [Pd(MeCN)₄][BF₄]₂ as a Pd(II) source with weakly coordinating auxiliary ligands²³ and anions.²⁴ NMR monitoring, performed in CD₃CN for solubility reasons, revealed similarly complicated reaction mixtures (Figure 3); however, a single product reproducibly crystallised. This product, confirmed to be the cationic bis(chelate) **6b** by X-ray crystallography (Scheme 3), produced an identical mixture when it was redissolved in CD₃CN. The spectra recorded in

CD₃OD and dms_o-d₆ exhibited similarly complicated patterns, but the isomer ratios varied (see the SI). Upon increasing the temperature, the ³¹P{¹H} NMR spectra changed: the number of the NMR resonances remained the same but their positions and relative intensities slightly changed (see the SI). All this suggests hemilabile coordination of the hybrid phosphine ligand.

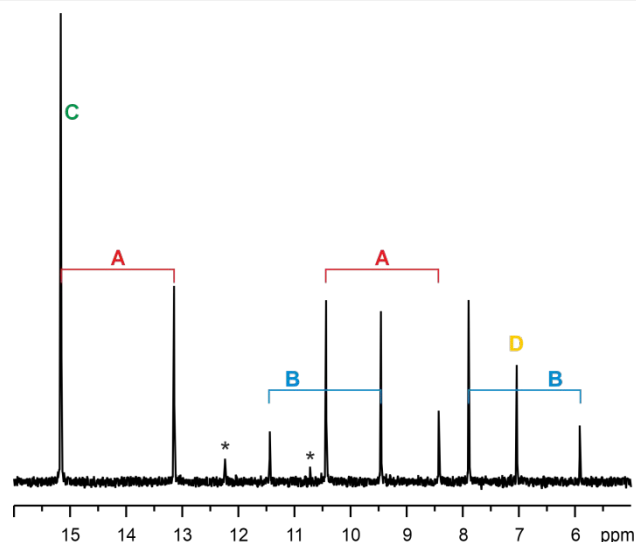


Figure 3 ³¹P{¹H} NMR spectrum (162 MHz, 25 °C) of crystalline **6b** dissolved in CD₃CN, with the observed signals tentatively assigned to four isomeric species. The data are quoted in the Experimental section. Asterisks denote additional unidentified signals.

The course of complexation reactions involving the hybrid phosphine **1** and, accordingly, the NMR signatures reflect the stereochemical complexity of the system. The structure of **5** combines a stereogenic carbon atom with an axially chiral ferrocene unit, whose conformation is fixed as a result of P,N-chelate coordination. Consequently, the compound can form four stereoisomers that aggregate into two diastereomeric pairs, giving rise to two sets of signals in the ¹H and ¹³C{¹H} NMR spectra and two separate ³¹P{¹H} NMR resonances (singlets).

Bis(chelate) complexes **6a** and **6b** contain two stereogenic carbon atoms and two axial-chiral ferrocene units and, correspondingly, the signals of four diastereoisomers are detected in the ³¹P{¹H} NMR spectrum (Figure 3). Crystallisation affords the most stable and/or the least soluble species. After dissolution, however, the system may undergo equilibration, regenerating the product mixture. Such behaviour possibly implies solvent-dependent hemilabile coordination of **1**, which enables conformational changes at the ferrocene unit (*S*_{ax} ↔ *R*_{ax}) *via* a decoordination/coordination sequence, whereas the configuration at the stereogenic carbon atoms remains expectedly unchanged.

Chelate complex **5** (Figure 4) crystallised in solvated form in the triclinic space group *P*-1, where the pair of (*R*,*R*_{ax}) and (*S*,*S*_{ax}) stereoisomers present in the unit cell is assembled into a centrosymmetric dimeric array *via* O-H...Cl hydrogen bridges (see the SI). The coordination environment of the Pd(II) ion is essentially planar,²⁵ and the Pd-donor distances fall within the normal ranges;²⁶ the elongation of the Pd1–Cl1 bond (relative to Pd1–Cl2) can be attributed to the strong *trans* influence of

Downloaded on 05 June 2016 09:39:45 AM. This article is licensed under a Creative Commons Attribution-NonCommercial 3.0 Unported Licence.



the phosphine donor.²⁷ The interligand angles also remain near the ideal value (90°), with the ligand bite angle P1–Pd1–N1 being the widest (93°). The ferrocene unit adopts a staggered conformation with $\tau = 42.92(2)^\circ$ and the cyclopentadienyl rings are practically parallel (interplanar angle: $4.8(2)^\circ$).

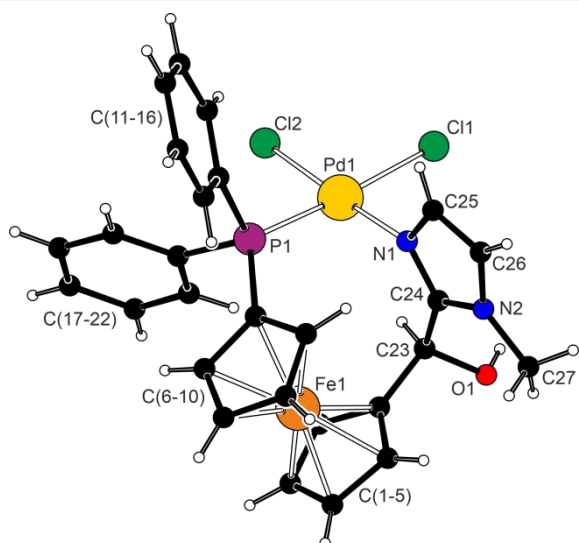


Figure 4 View of the complex molecule in the structure of **5**·2CHCl₃. Selected distances and angles (in Å and deg): Pd1–Cl1 2.3698(7), Pd1–Cl2 2.3008(8), Pd1–P1 2.2465(7), Pd1–N1 2.024(2), P1–Pd1–N1 93.23(7), Cl1–Pd1–Cl2 91.25(3), P1–Pd1–Cl2 87.00(3), N1–Pd1–Cl1 88.34(7), C23–O1 1.424(3), C1–C23–C24 114.7(2), C24–N1 1.328(3), C24–N2 1.355(4), N1–C24–N2 109.2(2). The displacement ellipsoid plot is available in the SI.

Despite the presence of various counteranions and differences in solvation, compounds **6a** and **6b** (Figure 5 and the SI) crystallised uniformly with their complex cations residing over the crystallographic inversion centres and with disordered CH(OH) moieties. As a result, the cations are composed of pairs of (*S*_{ax}) and (*R*_{ax}) ligands, each with the CH(OH) fragment in both (*S*)- and (*R*)-configurations (albeit not equally populated and with different ratios for the individual samples).

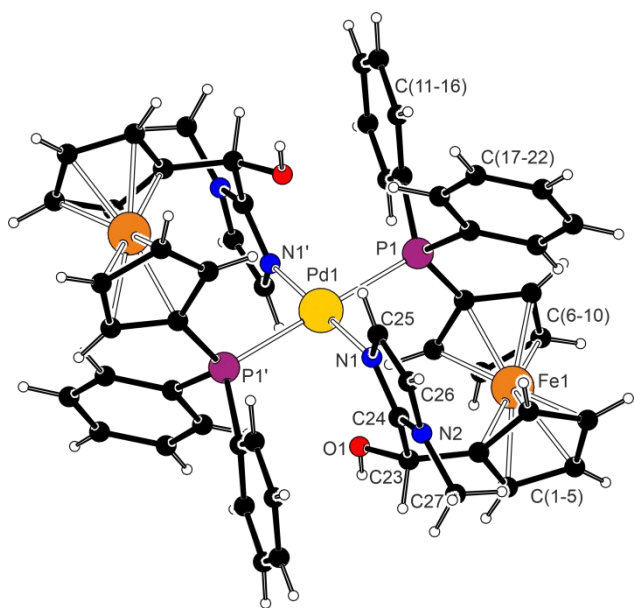
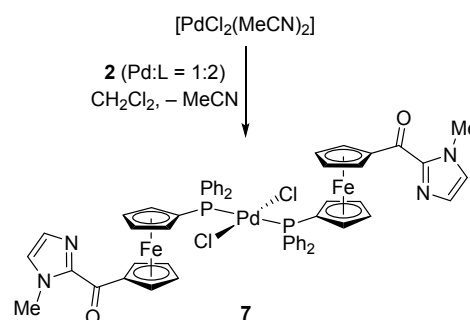


Figure 5 View of the complex molecule in the structure of **6b**·CH₂Cl₂. Only one position of the disordered OH group is shown for clarity. For a complete structure diagram, see the SI. Selected distances and angles (in Å and deg): Pd1–P1 2.3764(5), Pd1–N1 2.028(2), P1–Pd1–N1 90.44(6), P1–Pd1–N1' 89.57(6); C1–C23–C24 109.8(2), C24–N1 1.334(3), C24–N2 1.351(3), N1–C24–N2 109.9(2). The prime-labelled atoms are generated by the inversion operation.

The imposed crystallographic symmetry dictates a *trans*-P,P' arrangement and renders the central {PdP₂N₂} fragment ideally planar. The interligand angles in **6b**·CH₂Cl₂ differ only marginally from 90° (Figure 5). Compared with **5**, the bis(chelate) complex has a longer Pd1–P1 bond (by 0.13 Å), which can be attributed to antisymbiosis²⁸ of the soft phosphine moieties and, probably, to increased steric crowding. In contrast, the Pd1–N1 distance is practically unchanged, and the imidazole retains a position perpendicular to the coordination plane. The ferrocene units assume an intermediate conformation with $\tau = 53.0(2)^\circ$ (near the 1,2' arrangement²⁹), and their cyclopentadienyl rings are close to parallel (dihedral angle: $2.7(2)^\circ$). The parameters obtained for **6a**·4CHCl₃·2CH₃OH are similar (see the SI).

The interaction of [PdCl₂(MeCN)₂] with 1 equiv. of ketone **2** also led to product mixtures. Typically, several species were detected by ³¹P{¹H} NMR, and the composition of the mixture varied somewhat depending on the experimental conditions. Changing the Pd(II) source to [PdCl₂(cod)] (cod = cycloocta-1,5-diene) had no beneficial effect. However, when the amount of **2** was increased to 2 equiv. per palladium, the reaction cleanly produced the bis(phosphine) complex [PdCl₂(**2**-κP)₂] (**7**) (Scheme 4).



Scheme 4 Synthesis of bis(phosphine) complex **7**.

This behaviour is consistent with the greater rigidity of ligand **2**, where the rotation of the imidazole pendant can be hindered by the tendency of the carbonyl group to remain coplanar and conjugated with both the cyclopentadienyl ring and the terminal imidazole moiety. In addition, the presence of an electron-withdrawing carbonyl linker may weaken the ability of the imidazole nitrogen to act as a donor, thereby reducing the ligand's tendency to form P,N-chelate species and/or lowering their stability, especially when the carbonyl oxygen can compete as an additional donor with the imidazole nitrogen.³⁰ Unfortunately, reaction tests performed with **2** were complicated by the formation of black intractable solids, especially during extended reaction times and crystallisation, which precluded the isolation of other possible compounds present in the reaction mixtures. Complex **7** thus remains the sole compound isolated from the **2**–Pd system.

Downloaded from https://pubs.rsc.org on 05/06/2019 09:39:45 AM. This article is licensed under a Creative Commons Attribution-NonCommercial 3.0 Unported Licence.



In line with the P-monodentate coordination of the phosphine ligand in complex **7**, which allows rotation of the cyclopentadienyl rings along the axis of the ferrocene unit, the ^1H and $^{13}\text{C}\{^1\text{H}\}$ NMR spectra displayed only four signals due to the ferrocene CH groups. However, the $^{13}\text{C}\{^1\text{H}\}$ NMR signals of the carbon atoms showing scalar coupling with the phosphorus were observed as characteristic virtual triplets arising in the second-order ABX spin systems $^{13}\text{C}(\text{X})\text{--}^{31}\text{P}(\text{A})\text{--}\text{Pd}\text{--}^{31}\text{P}(\text{B})\text{--}^{12}\text{C}$ (Figure 6).³¹ The $^{31}\text{P}\{^1\text{H}\}$ NMR signal was detected at δ_{P} 14.7 (in CDCl_3).

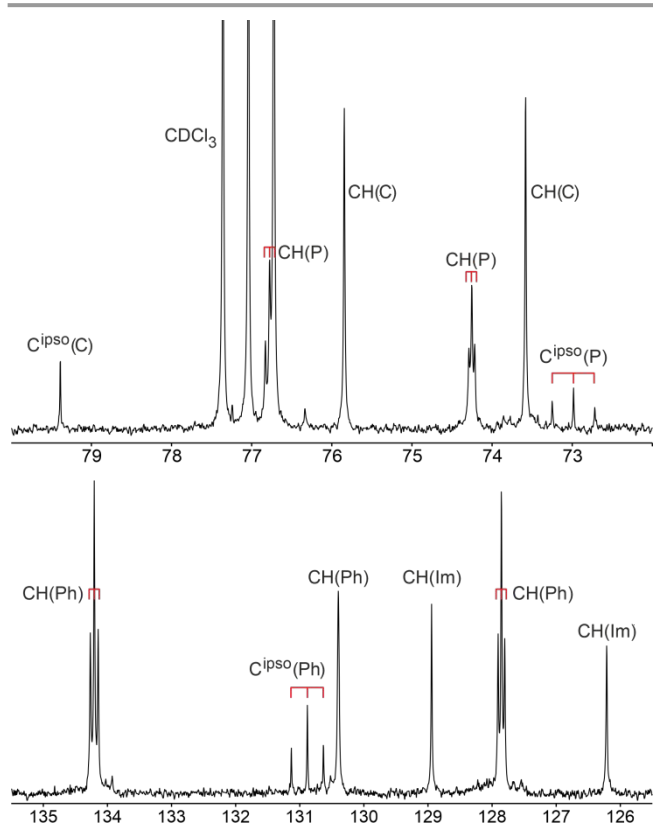


Figure 6 Sections of the $^{13}\text{C}\{^1\text{H}\}$ NMR spectrum of complex **7** (400 MHz, CDCl_3) showing the ferrocene (top) and phenyl (bottom) resonances. The signals are assigned to the CH and C^{ipso} carbons in phosphinylated (P) and CO-substituted (C) cyclopentadienyl rings, phenyl rings (Ph), and imidazole (Im) moieties. The second-order multiplets are indicated in red.

Compound **7** crystallised as a chloroform solvate $\mathbf{7}\cdot 2\text{CHCl}_3$ in the acentric space group $P2_12_12_1$. Nevertheless, structure determination revealed a symmetrical arrangement around Pd with *anti*-arranged ligands mimicking inversion symmetry (Figure 7). The palladium and its four ligating atoms are coplanar within ≈ 0.06 Å. The Pd–P and Pd–Cl bond distances are similar to those determined for *trans*- $[\text{PdCl}_2(\text{FcPPh}_2\text{-}\kappa\text{P})_2]$ ³² and analogous complexes obtained from the functional ferrocene phosphines, Ph_2PfcY (Fc = ferrocenyl; fc = ferrocene-1,1'-diyl),³³ and the interligand angles are $85\text{--}95^\circ$. In contrast to the chelate complexes discussed above, the two ferrocene units in **7** adopt more open conformations, with $\tau = 82.5(2)^\circ$ (Fe1) and $-86.9(2)^\circ$ (Fe2), while remaining negligibly tilted ($3.4(2)^\circ$ and $4.6(2)^\circ$). The two ligands mainly differ in positions of their heterocyclic pendants: the imidazole rings are rotated by

$9.3(2)^\circ$ (Fe1) and $34.9(2)^\circ$ (Fe2), and their connecting C–O units are twisted by $9.7(2)^\circ$ (Fe1) and $2.9(2)^\circ$ (Fe2) relative to the parent cyclopentadienyl rings C(1–5) and C(31–35), respectively.

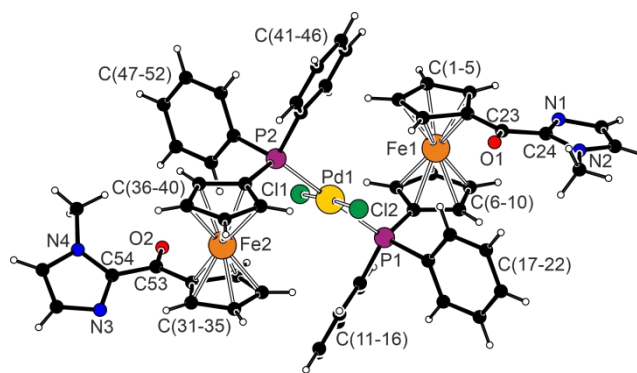
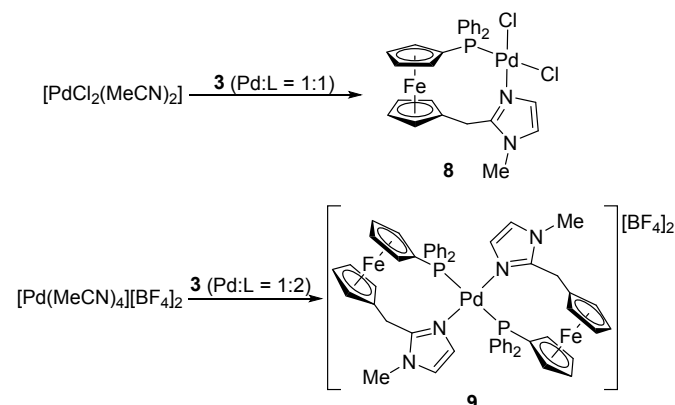


Figure 7 View of the complex molecule in the structure of $\mathbf{7}\cdot 2\text{CHCl}_3$. Selected distances and angles (in Å and deg): Pd1–P1 2.3441(7), Pd1–P2 2.3542(7), Pd1–Cl1 2.2956(7), Pd1–Cl2 2.3061(7), P1–Pd1–Cl1 84.79(2), P1–Pd1–Cl2 94.53(3), P2–Pd1–Cl1 93.69(3), P2–Pd1–Cl2 87.11(2); C23–O1 1.224(4), C1–C23–C24 119.0(3), C53–O2 1.226(4), C31–C53–C54 118.3(3), C24–N1 1.328(4), C24–N2 1.373(4), N1–C24–N2 111.2(3), C54–N3 1.323(4), C54–N4 1.373(4), N3–C54–N4 111.6(3).

Complexation reactions with **3** bearing a methylene spacer resembled those of alcohol **1**, in line with the flexible and non-conjugated nature of the methylene linker. However, owing to the absence of a chiral centre, they appeared simpler from a stereochemical viewpoint (Scheme 5). The reaction of **3** with $[\text{PdCl}_2(\text{MeCN})_2]$ in equimolar amounts smoothly produced P,N-chelate complex **8**, whereas a similar reaction with 2 equiv. of the phosphine afforded a mixture of uncoordinated **3** and two complexes, presumably compound **8** and the bis(chelate) complex $[\text{Pd}(\mathbf{3}\text{-}\kappa^2\text{P},\text{N})_2]\text{Cl}_2$ (as two stereoisomers; *vide supra*). Increasing the amount of **3** by 10 mol.% (to 2.2 equiv. per Pd) suppressed the formation of **8**, while the amount of $[\text{Pd}(\mathbf{3}\text{-}\kappa^2\text{P},\text{N})_2]\text{Cl}_2$ increased (some ligand remained unreacted). Upon changing the Pd(II) source to $[\text{Pd}(\text{MeCN})_4][\text{BF}_4]_2$, the reaction with 2 equiv. of **3** selectively produced the bis(chelate) complex **9** (Scheme 5).



Scheme 5 Synthesis of complexes **8** and **9**.

Owing to the fixed conformation of the ferrocene unit, compound **8** results as a mixture of (S_{ax}) and (R_{ax}) enantiomers,



which exhibit an identical NMR signature (*e.g.*, eight signals due to the ferrocene CH group in the ^1H and $^{13}\text{C}\{^1\text{H}\}$ NMR spectra and a pair of ^1H NMR signals of the diastereotopic CH_2 protons). The ^{31}P NMR resonance was detected at δ_{P} 22.3 (in CDCl_3). Conversely, complex **9** is obtained as a pair of ($R_{\text{ax}}, R_{\text{ax}}$)/($S_{\text{ax}}, S_{\text{ax}}$) and ($R_{\text{ax}}, S_{\text{ax}}$)/($S_{\text{ax}}, R_{\text{ax}}$) diastereoisomers (formally corresponding to racemic and *meso* forms), with ^{31}P NMR signals at δ_{P} 15.3 and 12.5 in a $\approx 7:3$ ratio (not assigned).

Compound **8** crystallises as a racemate (space group $P2_1/n$). The structure of solvate **8**· 2CHCl_3 (Figure 8) reveals undistorted square coordination around palladium, where the Pd and ligating atoms are coplanar within ≈ 0.04 Å and the interligand angles remain near 90° . The Pd-donor distances are similar to those determined for **5**· 2CHCl_3 , with the Pd–Cl bond *trans* to the phosphine donor moiety being characteristically elongated (> 0.1 Å) because of *trans* influence. The ferrocene unit has an approximately 1,2' conformation ($\tau = -54.9(1)^\circ$; tilt: $3.8(1)^\circ$), and the $\text{CH}_2\text{Im}^{\text{Me}}$ pendant is oriented so that the imidazole ring intersects the {PdL₄} plane at an angle of $73.84(7)^\circ$.

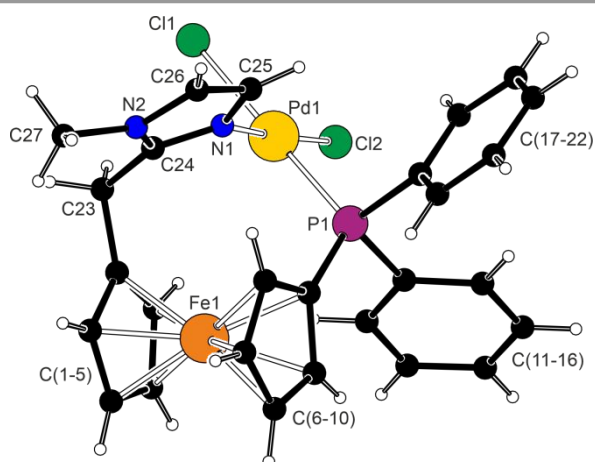


Figure 8 View of the complex molecule in the structure of **8**· 2CHCl_3 . Selected distances and angles (in Å and deg): Pd1–P1 2.2364(5), Pd1–N1 2.029(1), Pd1–Cl1 2.3810(5), Pd1–Cl2 2.2776(5), P1–Pd1–N1 89.84(4), P1–Pd1–Cl1 88.44(4), Cl1–Pd1–Cl2 90.89(2), C1–C23–C24 115.2(1), C24–N1 1.331(2), C24–N2 1.350(2), N1–C24–N2 109.2(2).

Complex **9** crystallised as solvate **9**· CH_2Cl_2 (Figure 9) with the complex cations and solvent molecules lying over the crystallographic inversion centres (space group $P2_1/n$). In many respects, the structure resembles that of **6b**· CH_2Cl_2 : the coordination sphere around the palladium atom is planar, all interligand angles are $\approx 90^\circ$, and the imidazole unit is perpendicular to the coordination plane (dihedral angle: $88.86(7)^\circ$). The structure is stabilised by intramolecular $\pi\cdots\pi$ interactions³⁴ between the imidazole ring from one ligand and the phenyl ring C(11–12) from the other (interplanar angle: $11.81(8)^\circ$; distance between the ring centroids: $3.5993(3)^\circ$). Notably, this interaction causes the pivotal P1–C11 bond to bend from the mean phenyl ring plane (by $6.34(7)^\circ$; *cf.* $2.60(7)^\circ$ for P1–C17 and the other phenyl ring).

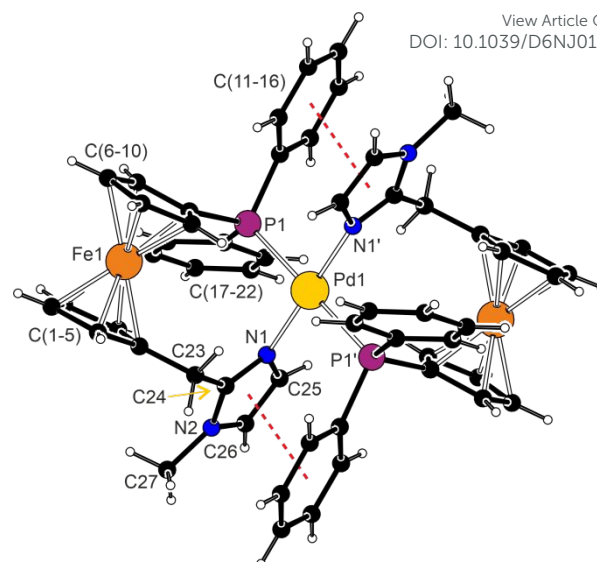
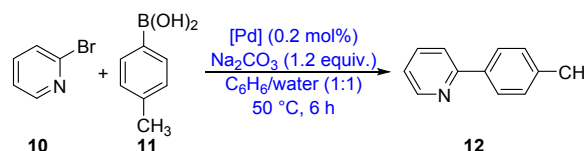


Figure 9 View of the complex molecule in the structure of **9**· CH_2Cl_2 . Selected distances and angles (in Å and deg): Pd1–P1 2.3678(4), Pd1–N1 2.038(1), P1–Pd1–N1 90.76(3), P1–Pd1–N1' 89.24(3), C1–C23–C24 110.8(1), C24–N1 1.335(2), C24–N2 1.352(2), N1–C24–N2 109.3(1). The prime-labelled atoms are generated by crystallographic inversion. The $\pi\cdots\pi$ interaction is indicated by a red dotted line.

Catalytic evaluation

Following early reports in the late 1970s,³⁵ the Suzuki–Miyaura cross-coupling of organoboron reagents and organic halides has rapidly developed into a powerful synthetic tool with many practical applications.³⁶ Despite enormous progress, however, some challenges remain, such as the coupling of heteroaryl substrates.³⁷ We used this type of reaction, namely the Suzuki–Miyaura cross-coupling of 2-bromopyridine (**10**) with 4-tolylboronic acid (**11**) (Scheme 6), to catalytically evaluate the prepared P,N-chelate complexes **5** and **8**, and to compare them with $[\text{PdCl}_2(\text{C-}\kappa^2\text{P},\text{N})]$ (see Figure 1), compounds containing the related bis(phosphine) ligands, *viz.* $[\text{PdCl}_2(\text{dppf-}\kappa^2\text{P},\text{P}')]]$ (dppf = 1,1'-bis(diphenylphosphino)ferrocene), $[\text{PdCl}_2(\text{Ph}_2\text{PfcCH}_2\text{PPh}_2\text{-}\kappa^2\text{P},\text{P}')]]$,³⁸ and the triphenylphosphine complex $[\text{PdCl}_2(\text{PPh}_3)_2]$. The coupling reactions were performed in benzene–water at 50°C using 0.2 mol% Pd catalyst and Na_2CO_3 as the base (1.2 equiv.) and were monitored by NMR spectroscopy using the methyl substituent as a spectroscopic probe.



Scheme 6 Pd-catalysed Suzuki–Miyaura cross-coupling of 2-bromopyridine (**10**) with 4-tolylboronic acid (**11**). The boronic acid was used in excess (1.2 equiv. relative to **10**).

The results presented in Table 1 indicate the superior catalytic performance of the previously reported⁴ P,N-chelate complex $[\text{PdCl}_2(\text{C-}\kappa^2\text{P},\text{N})]$, achieving an 81% yield of the targeted coupling product **12**. Somewhat lower yields were obtained with **8** and $[\text{PdCl}_2(\text{dppf-}\kappa^2\text{P},\text{P}')]]$, whereas the remaining chelate complexes **5** and $[\text{PdCl}_2(\text{Ph}_2\text{PfcCH}_2\text{PPh}_2\text{-}\kappa^2\text{P},\text{P}')]]$ were less

Downloaded on 05 June 2016 09:39:45 AM. This article is licensed under a Creative Commons Attribution-NonCommercial 3.0 Unported Licence.

efficient. The worst result was obtained with $[\text{PdCl}_2(\text{PPh}_3)_2]$ featuring monodentate triphenylphosphine ligands.

The reaction mixtures retained their initial colours (yellow or yellow-orange due to the catalyst) throughout the reaction; no formation of palladium black was observed. This suggested the homogeneous nature of the catalyst,³⁹ which was further corroborated by the mercury poisoning test.⁴⁰ The reaction performed with complex **8** as the representative catalyst and elemental mercury afforded the coupling product with a practically unchanged yield (63%).

Table 1 Summary of the catalytic results.^a

Catalyst	Yield of 12 [%]	Catalyst	Yield of 12 [%]
5	56	$[\text{PdCl}_2(\text{dppf})]$	73
8	66	$[\text{PdCl}_2(\text{Ph}_2\text{PfcCH}_2\text{PPh}_2)]$	55
$[\text{PdCl}_2(\text{C})]$	81	$[\text{PdCl}_2(\text{PPh}_3)_2]$	20

^a For conditions, see the text. The yields were determined by ¹H NMR spectroscopy and represent an average of two independent runs, where the yield differed by less than 5%.

Conclusions

Overall, this study reports the preparation of three hybrid phosphinoferrrocene ligands bearing an additional 1-methyl-1*H*-imidazol-2-yl substituent. This N-donor pendant is connected *via* different bridging units, *viz.* CH(OH), C=O, and CH₂, which significantly influence the coordination behaviour of the resulting P,N-hybrid ligands. While the compounds featuring the flexible CH(OH) and CH₂ bridges readily form P,N-chelate complexes, the similar coordination of their C=O-bridged analogue is compromised by the tendency of the carbonyl group to remain conjugated with the cyclopentadienyl and imidazole moieties and, possibly, also by the changed basicity of the imidazole nitrogen. Additional features that differentiate the linkers and, consequently, the ligands and their complexes, are their stereochemical properties (chirality) and different abilities to form intermolecular interactions, typically hydrogen bonds. Reactivity tests performed with these ligands suggest their hemilabile coordination to Pd(II), which enables exchange between the stereoisomers and their mutual interconversions *via* conformational changes. The complexes exhibit favourable catalytic properties that render them attractive (pre)catalysts for Suzuki–Miyaura reactions of difficult-to-couple substrates.

Experimental

Materials and methods

All syntheses were performed under a nitrogen atmosphere using the standard Schlenk techniques.⁴¹ 1-Bromo-1'-(diphenylphosphino)ferrocene (**4**),⁸ the corresponding borane adduct **4**·BH₃,⁴² $[\text{PdCl}_2(\text{Ph}_2\text{PfcCH}_2\text{PPh}_2-\kappa^2P,P')]$,³⁸ and $[\text{PdCl}_2(\text{dppf}-\kappa^2P,P')]$ ⁴³ were synthesised by following the literature procedures. Other chemicals were purchased from commercial suppliers (Sigma–Aldrich and TCI) and were used as received. Anhydrous and oxygen-free tetrahydrofuran (THF), dichloromethane, toluene and diethyl ether were obtained

from a PureSolv MD5 solvent purification system (Innovative Technology, Inc.). The solvents for column chromatography and crystallisations were used without purification (analytical grade; Lach-Ner, Czech Republic).

The NMR spectra were recorded on Bruker Avance III 400, Avance NEO 400, and Avance III 600 spectrometers at 25 °C. Chemical shifts (δ /ppm) are given relative to internal tetramethylsilane (¹H and ¹³C NMR) and external 85% aqueous H₃PO₄ (³¹P NMR). The signals are labelled as s (singlet), d (doublet), t (triplet), q (quartet), and m (multiplet),⁴⁴ with the prefix v added for virtual multiplets due to the magnetically nonequivalent hydrogen atoms at the substituted cyclopentadienyl rings (C₅H₄). Electrospray ionisation mass spectra (ESI MS) were obtained on a Bruker QTOF Micro spectrometer using samples dissolved in methanol or acetonitrile (HPLC grade). Elemental analyses were performed on a PE 2400 Series II CHNS/O elemental analyser (Perkin Elmer). Some of the compounds were obtained as crystallising (solidifying) oils, which tended to retain the solvents used during isolation. The amount of residual solvent was verified by NMR analysis and considered during the following synthetic steps, especially during the preparation of Pd(II) complexes. Details of structure determination are available in the SI.

Syntheses

Preparation of alcohol 1. An oven-dried 25 mL flask was charged with bromide **4** (449 mg, 1.0 mmol) and anhydrous THF (10 mL) under nitrogen, and the solution was cooled to –78 °C using a dry ice/ethanol bath. *n*-Butyllithium (0.44 mL of 2.5 M solution in THF, 1.1 mmol) was introduced, and the resulting mixture was stirred for 45 min, during which time an orange precipitate formed. A solution of 1-methyl-1*H*-imidazole-2-carboxaldehyde (121 mg, 1.1 mmol) in dry THF (5 mL) was added, and the reaction mixture was stirred with cooling for 15 min and then at room temperature for another 2 h. During this period, the orange precipitate completely dissolved. The reaction was terminated by the addition of distilled water (20 mL) and ethyl acetate (30 mL). The orange organic layer was separated, washed with brine (20 mL), dried over MgSO₄, filtered, and concentrated under vacuum. The orange residue was dissolved in dichloromethane (40 mL) and evaporated with chromatographic alumina. The crude preadsorbed material was transferred onto the top of an alumina column packed with hexane–ethyl acetate (3:1). Elution with the same solvent mixture led to the separation of the first yellow band, which contained nonpolar byproducts (66 mg). The second red band, eluted with hexane–ethyl acetate (1:1), afforded ketone **2** as a red oil (3 mg, 1%). Finally, the eluent was changed to dichloromethane–methanol (20:1) to elute the product. The subsequent evaporation produced alcohol **1** as an orange solid. Yield: 280 mg (58%). The crystal yield for structure determination was obtained from acetonitrile–diethyl ether.

¹H NMR (400 MHz, CDCl₃): δ 3.62 (s, 3 H, CH₃), 4.04–4.08 (m, 2 H, C₅H₄), 4.11–4.16 (m, 2 H, C₅H₄), 4.16–4.19 (m, 1 H, C₅H₄), 4.28–4.30 (m, 1 H, C₅H₄), 4.40–4.45 (m, 2 H, C₅H₄), 5.62 (s, 1 H, CHOH), 6.75 (d, *J* = 1.2 Hz, 1 H, C₃H₂N₂), 6.89 (d, *J* = 1.2 Hz, 1 H, C₃H₂N₂), 7.28–7.45 (m, 10 H, PPh₂). The signal of CHOH was not

Downloaded from www.rsc.org on 05/06/2016 09:39:45 AM
 This article is licensed under a Creative Commons Attribution-NonCommercial 3.0 Unported Licence.


observed. $^{31}\text{P}\{^1\text{H}\}$ NMR (162 MHz, CDCl_3) δ -16.9 (s, PPh_2). $^{13}\text{C}\{^1\text{H}\}$ NMR (100.6 MHz, CDCl_3): δ 33.25 (s, CH_3), 66.19 (s, CHOH), 67.56 (s, $\text{CH C}_5\text{H}_4$), 68.32 (s, $\text{CH C}_5\text{H}_4$), 69.23 (s, $\text{CH C}_5\text{H}_4$), 69.45 (s, $\text{CH C}_5\text{H}_4$), 71.70 (d, $J_{\text{PC}} = 3$ Hz, $\text{CH C}_5\text{H}_4$), 71.86 (d, $J_{\text{PC}} = 4$ Hz, $\text{CH C}_5\text{H}_4$), 73.12 (d, $J_{\text{PC}} = 12$ Hz, $\text{CH C}_5\text{H}_4$), 73.94 (d, $J_{\text{PC}} = 16$ Hz, $\text{CH C}_5\text{H}_4$), 76.21 (d, $J_{\text{PC}} = 5$ Hz, $\text{C}^{\text{ipso}}\text{-P C}_5\text{H}_4$), 90.65 (s, $\text{C}^{\text{ipso}}\text{-C C}_5\text{H}_4$), 121.69 (s, $\text{CH C}_3\text{H}_2\text{N}_2$), 126.92 (s, $\text{CH C}_3\text{H}_2\text{N}_2$), 128.19 (s, CH PPh_2), 128.26 (s, CH PPh_2), 128.58 (s, CH PPh_2), 128.72 (s, CH PPh_2), 133.32 (d, $J_{\text{PC}} = 19$ Hz, CH PPh_2), 133.68 (d, $J_{\text{PC}} = 19$ Hz, CH PPh_2), 138.44 (d, $J_{\text{PC}} = 9$ Hz, $\text{C}^{\text{ipso}}\text{ PPh}_2$), 138.85 (d, $J_{\text{PC}} = 9$ Hz, $\text{C}^{\text{ipso}}\text{ PPh}_2$), 148.32 (s, $\text{C}^{\text{ipso}}\text{ C}_3\text{H}_2\text{N}_2$). HRMS (ESI+), m/z calc. for $\text{C}_{27}\text{H}_{26}\text{FeN}_2\text{OP}$ ($[\text{M} + \text{H}]^+$): 481.1126; found: 481.1148. Anal. Calc. for $\text{C}_{27}\text{H}_{25}\text{FeN}_2\text{OP}$ (480.3): C 67.52, H 5.25, N 5.83%. Found: C 67.40, H 5.14, N 5.94%.

Synthesis of adduct 1-BH₃. Bromide 4-BH₃ (2.776 g, 6.0 mmol) was dissolved in anhydrous THF (60 mL), and the solution was cooled to -78 °C using a dry ice/ethanol bath. *n*-Butyllithium (2.6 mL of 2.5 M solution in THF, 6.6 mmol) was added, and the mixture was stirred for 45 min (an orange precipitate formed during this time). Next, a solution of 1-methyl-1*H*-imidazole-2-carboxaldehyde (0.727 g, 6.6 mmol) in dry THF (20 mL) was added, and the resulting mixture was stirred under cooling for 15 min and then at room temperature for 2 h. The orange precipitate dissolved, and another orange–yellow solid separated from the reaction mixture. The reaction was terminated by adding distilled water (75 mL) and ethyl acetate (150 mL). The orange organic layer was separated, washed with brine (60 mL), dried over MgSO_4 , filtered, and concentrated under vacuum. The orange residue was dissolved in dichloromethane (100 mL) and evaporated with chromatographic alumina. The preadsorbed product was transferred onto the top of an alumina column packed with hexane–ethyl acetate (3:1). Elution with the same solvent mixture led to the development of the first yellow band containing nonpolar byproducts (629 mg). A second red band was eluted with hexane–ethyl acetate (1:1), which produced 2-BH₃ as a red oil after evaporation (15 mg, 1%). Eventually, the mobile phase was changed to dichloromethane–methanol (50:1) to elute the targeted product. After evaporation, compound 1-BH₃ was obtained as an orange solid. Yield: 2.003 g (68%).

^1H NMR (400 MHz, CDCl_3): δ 0.72–1.80 (br m, 3 H, BH_3), 3.58 (s, 3 H, CH_3), 4.01–4.08 (m, 2 H, C_5H_4), 4.16–4.20 (m, 1 H, C_5H_4), 4.34–4.38 (m, 1 H, C_5H_4), 4.38–4.44 (m, 2 H, C_5H_4), 4.52–4.56 (m, 1 H, C_5H_4), 4.56–4.59 (m, 1 H, C_5H_4), 5.55 (s, 1 H, CHOH), 6.73 (d, $J = 1.2$ Hz, 1 H, $\text{C}_3\text{H}_2\text{N}_2$), 6.87 (d, $J = 1.2$ Hz, 1 H, $\text{C}_3\text{H}_2\text{N}_2$), 7.35–7.51 (m, 6 H, PPh_2), 7.52–7.65 (m, 4 H, PPh_2). $^{31}\text{P}\{^1\text{H}\}$ NMR (162 MHz, CDCl_3) δ 15.7 (br s, $\text{PPh}_2\text{-BH}_3$). $^{13}\text{C}\{^1\text{H}\}$ NMR (100.6 MHz, CDCl_3): δ 33.27 (s, CH_3), 65.58 (s, CHOH), 68.24 (s, $\text{CH C}_5\text{H}_4$), 68.87 (s, $\text{CH C}_5\text{H}_4$), 69.26 (d, $J_{\text{PC}} = 69$ Hz, $\text{C}^{\text{ipso}}\text{-P C}_5\text{H}_4$), 69.76 (s, $\text{CH C}_5\text{H}_4$), 70.16 (s, $\text{CH C}_5\text{H}_4$), 73.04 (d, $J_{\text{PC}} = 8$ Hz, $\text{CH C}_5\text{H}_4$), 73.27 (d, $J_{\text{PC}} = 8$ Hz, $\text{CH C}_5\text{H}_4$), 73.40 (d, $J_{\text{PC}} = 10$ Hz, $\text{CH C}_5\text{H}_4$), 73.61 (d, $J_{\text{PC}} = 10$ Hz, $\text{CH C}_5\text{H}_4$), 91.21 (s, $\text{C}^{\text{ipso}}\text{-C C}_5\text{H}_4$), 121.71 (s, $\text{CH C}_3\text{H}_2\text{N}_2$), 126.74 (s, $\text{CH C}_3\text{H}_2\text{N}_2$), 128.41 (s, CH PPh_2), 128.51 (s, CH PPh_2), 130.92 (d, $J_{\text{PC}} = 3$ Hz, CH PPh_2), 130.97 (d, $J_{\text{PC}} = 3$ Hz, CH PPh_2), 131.04 (d, $J_{\text{PC}} = 59$ Hz, $\text{C}^{\text{ipso}}\text{ PPh}_2$), 131.17 (d, $J_{\text{PC}} = 59$ Hz, $\text{C}^{\text{ipso}}\text{ PPh}_2$), 132.57 (d, $J_{\text{PC}} = 10$ Hz, CH PPh_2), 132.67 (d, $J_{\text{PC}} =$

10 Hz, CH PPh_2), 148.53 (s, $\text{C}^{\text{ipso}}\text{ C}_3\text{H}_2\text{N}_2$). HRMS (ESI+), m/z calc. for $\text{C}_{27}\text{H}_{29}\text{BFeN}_2\text{OP}$ ($[\text{M} + \text{H}]^+$): 495.1465; found: 495.1468. Anal. Calc. for $\text{C}_{27}\text{H}_{28}\text{BFeN}_2\text{OP}\cdot 0.1\text{CH}_2\text{Cl}_2$ (502.7): C 64.76, H 5.66, N 5.57%. Found: C 64.91, H 5.49, N 5.35%.

Synthesis of 2-BH₃. A 25 mL flask was charged with 1-BH₃ (247 mg, 0.5 mmol), MnO_2 (869 mg, 10 mmol), and anhydrous dichloromethane (10 mL). The resulting dark mixture was stirred at room temperature for 1 h and filtered through a Celite pad on a frit. The frit was washed with dichloromethane until the filtrate became colourless. The combined filtrate was evaporated under vacuum, and the residue was dissolved in a minimal amount of dichloromethane–methanol (20:1) and transferred onto the top of a silica gel column. Elution with the same solvent resulted in the formation of a red band, which was collected and evaporated to produce ketone 2-BH₃ as a red solid. Yield: 176 mg (71%).

^1H NMR (400 MHz, CDCl_3): δ 0.68–1.82 (br m, 3 H, BH_3), 3.99 (s, 3 H CH_3), 4.45 (vt, $J' = 1.9$ Hz, 2 H, C_5H_4), 4.47–4.54 (m, 4 H, C_5H_4), 5.31 (vt, $J' = 2.0$ Hz, 2 H, C_5H_4), 7.02 (d, $J = 1.0$ Hz, 1 H, $\text{C}_3\text{H}_2\text{N}_2$), 7.13 (d, $J = 1.0$ Hz, 1 H, $\text{C}_3\text{H}_2\text{N}_2$), 7.32–7.44 (m, 4 H, PPh_2), 7.43–7.50 (m, 2 H, PPh_2), 7.51–7.60 (m, 4 H, PPh_2). $^{31}\text{P}\{^1\text{H}\}$ NMR (162 MHz, CDCl_3) δ 15.8 (br s, $\text{PPh}_2\text{-BH}_3$). $^{13}\text{C}\{^1\text{H}\}$ NMR (100.6 MHz, CDCl_3): δ 36.31 (s, CH_3), 70.61 (d, $J_{\text{PC}} = 67$ Hz, $\text{C}^{\text{ipso}}\text{-P C}_5\text{H}_4$), 73.44 (s, $\text{CH C}_5\text{H}_4$), 74.28 (d, $J_{\text{PC}} = 10$ Hz, $\text{CH C}_5\text{H}_4$), 74.50 (d, $J_{\text{PC}} = 7$ Hz, $\text{CH C}_5\text{H}_4$), 74.51 (s, $\text{CH C}_5\text{H}_4$), 79.40 (s, $\text{C}^{\text{ipso}}\text{-C C}_5\text{H}_4$), 126.24 (s, $\text{CH C}_3\text{H}_2\text{N}_2$), 128.48 (d, $J_{\text{PC}} = 10$ Hz, CH PPh_2), 128.87 (s, $\text{CH C}_3\text{H}_2\text{N}_2$), 130.84 (d, $J_{\text{PC}} = 59$ Hz, $\text{C}^{\text{ipso}}\text{ PPh}_2$), 130.99 (d, $J_{\text{PC}} = 2$ Hz, CH PPh_2), 132.61 (d, $J_{\text{PC}} = 10$ Hz, CH PPh_2), 143.41 (s, $\text{C}^{\text{ipso}}\text{ C}_3\text{H}_2\text{N}_2$), 187.20 (s, $\text{C}=\text{O}$). HRMS (ESI+), m/z calc. for $\text{C}_{27}\text{H}_{27}\text{BFeN}_2\text{OP}$ ($[\text{M} + \text{H}]^+$): 493.1298; found: 493.1299. Anal. Calc. for $\text{C}_{27}\text{H}_{26}\text{BFeN}_2\text{OP}$ (492.1): C 65.89, H 5.33, N 5.69%. Found: C 65.98, H 5.30, N 5.65%.

Deprotection of 2-BH₃. A dry Schlenk flask was charged with 2-BH₃ (123 mg, 0.25 mmol) and 1,4-diazabicyclo[2.2.2]octane (dabco; 140 mg, 1.3 mmol). After three vacuum–nitrogen cycles, degassed toluene (1.5 mL) was introduced, and the resulting red solution was heated at 50 °C for 2 h. The solvent was removed under vacuum, and the residue was dissolved in a minimal amount of dichloromethane (5 mL) and evaporated with chromatographic silica gel. The crude preadsorbed product was loaded onto a silica gel column packed with hexane–ethyl acetate (3:1). Elution with the same solvent mixture resulted in the formation of a red band, which was collected and evaporated to produce 2 as a red solid. Yield: 99 mg (83%).

^1H NMR (400 MHz, CDCl_3): δ 4.02 (s, 3 H, CH_3), 4.09 (vt, $J' = 1.8$ Hz, 2 H, C_5H_4), 4.37 (vt, $J' = 1.8$ Hz, 2 H, C_5H_4), 4.44 (vt, $J' = 2.0$ Hz, 2 H, C_5H_4), 5.37 (vt, $J' = 2.0$ Hz, 2 H, C_5H_4), 7.02 (d, $J = 1.0$ Hz, 1 H, $\text{C}_3\text{H}_2\text{N}_2$), 7.15 (d, $J = 1.0$ Hz, 1 H, $\text{C}_3\text{H}_2\text{N}_2$), 7.28–7.36 (m, 10 H, PPh_2). $^{31}\text{P}\{^1\text{H}\}$ NMR (162 MHz, CDCl_3) δ -18.0 (s, PPh_2). $^{13}\text{C}\{^1\text{H}\}$ NMR (100.6 MHz, CDCl_3): δ 36.36 (s, CH_3), 72.96 (s, $\text{CH C}_5\text{H}_4$), 73.14 (d, $J_{\text{PC}} = 4$ Hz, $\text{CH C}_5\text{H}_4$), 73.93 (d, $J_{\text{PC}} = 1$ Hz, $\text{CH C}_5\text{H}_4$), 74.41 (d, $J_{\text{PC}} = 14$ Hz, $\text{CH C}_5\text{H}_4$), 78.19 (d, $J_{\text{PC}} = 9$ Hz, $\text{C}^{\text{ipso}}\text{-P C}_5\text{H}_4$), 78.99 (s, $\text{C}^{\text{ipso}}\text{-C C}_5\text{H}_4$), 126.04 (s, $\text{CH C}_3\text{H}_2\text{N}_2$), 128.18 (d, $J_{\text{PC}} = 7$ Hz, CH PPh_2), 128.57 (s, CH PPh_2), 128.71 (s, $\text{CH C}_3\text{H}_2\text{N}_2$), 133.47 (d, $J_{\text{PC}} = 20$ Hz, CH PPh_2), 138.56 (d, $J_{\text{PC}} = 10$ Hz, $\text{C}^{\text{ipso}}\text{ PPh}_2$), 143.68 (s, $\text{C}^{\text{ipso}}\text{ C}_3\text{H}_2\text{N}_2$), 187.20 (s, $\text{C}=\text{O}$). HRMS (ESI+), m/z calc. for $\text{C}_{27}\text{H}_{24}\text{FeN}_2\text{OP}$ ($[\text{M} + \text{H}]^+$): 479.0970; found: 479.0961. Anal. Calc.

Downloaded from www.rsc.org on 05/06/2016 09:39:45 AM. This article is licensed under a Creative Commons Attribution-NonCommercial 3.0 Unported Licence.



for C₂₇H₂₃FeN₂OP·0.1CH₂Cl₂ (486.8): C 66.86, H 4.80, N 5.75%. Found: C 67.28, H 5.01, N 5.33%.

Deoxygenation of 1-BH₃. Adduct 1-BH₃ (645 mg, 1.3 mmol) was dissolved in dry dichloromethane (15 mL) under nitrogen. Neat triethylsilane (3.1 mL, 20 mmol) followed by trifluoroacetic acid (1.5 mL, 20 mmol) were added dropwise, and the resulting brown–orange solution was stirred at room temperature overnight. Saturated aqueous NaHCO₃ (50 mL) was added, and the mixture was vigorously stirred for an additional 20 min. The organic layer was separated and washed successively with saturated aqueous NaHCO₃ (4 × 40 mL), distilled water (40 mL), and brine (40 mL), dried over MgSO₄, and evaporated. The residue was taken up with dichloromethane and purified by chromatography over alumina. Elution with pure dichloromethane removed a minor yellow band, which was discarded. The mobile phase was then changed to dichloromethane–methanol (75:1) to elute a second major yellow band, which was collected and evaporated under vacuum, leaving a 65:35 mixture of **3** and **3**-BH₃ as a yellow oil. Yield: 280 mg.

Selected characterisation data for **3**-BH₃. ¹H NMR (400 MHz, CDCl₃): δ 3.50 (s, 3 H, CH₃), 3.56 (s, 2 H, CH₂), ≈4.0 (m, 2 H, C₅H₄), 4.17 (vt, *J*' = 1.8 Hz, 2 H, C₅H₄), 4.37 (vq, *J*' = 1.9 Hz, 2 H, C₅H₄), 4.51 (vq, *J*' = 1.9 Hz, 2 H, C₅H₄); other signals could not be unambiguously identified because of overlaps with the resonances of the free phosphine. ³¹P{¹H} NMR (162 MHz, CDCl₃) δ 15.7 (br s, PPh₂-BH₃). HRMS (ESI+), *m/z* calc. for C₂₇H₂₆FeN₂P ([**3** + H]⁺): 465.1177; found: 465.1182; *m/z* calc. for C₂₇H₂₉BFeN₂P ([**3**-BH₃ + H]⁺): 479.1505; found: 479.1497.

Preparation of 3. A dry Schlenk flask was charged with the mixture of **3** and **3**-BH₃ from the preceding step (65:35, 280 mg) and 1,4-diazabicyclo[2.2.2]octane (334 mg, 3.0 mmol). After three vacuum–nitrogen cycles, degassed toluene (8 mL) was introduced, and the yellow reaction mixture was stirred at 60 °C for 3 h. Then, the mixture was concentrated under vacuum, and the residue was dissolved in a minimal amount of dichloromethane–methanol (20:1) and purified by chromatography on a silica gel column, eluting with the same solvent mixture. The first yellow band was collected and evaporated, leaving **3**·0.1CH₂Cl₂ as a yellow solid. Yield: 185 mg (30% over the two steps).

¹H NMR (400 MHz, CDCl₃): δ 3.48 (s, 3 H, CH₃), 3.59 (s, 2 H, CH₂), 3.98 (vt, *J*' = 1.8 Hz, 2 H, C₅H₄), 4.06 (vq, *J*' = 1.9 Hz, 2 H, C₅H₄), 4.09 (vt, *J*' = 1.9 Hz, 2 H, C₅H₄), 4.36 (vt, *J*' = 1.8 Hz, 2 H, C₅H₄), 6.71 (s, 1 H, C₃H₂N₂), 6.87 (s, 1 H, C₃H₂N₂), 7.27–7.33 (m, 6 H, PPh₂), 7.33–7.42 (m, 4 H, PPh₂). ³¹P{¹H} NMR (162 MHz, CDCl₃) δ 16.9 (s, PPh₂). ¹³C{¹H} NMR (100.6 MHz, CDCl₃): δ 27.34 (s, CH₂), 32.96 (s, CH₃), 69.07 (s, CH C₅H₄), 69.78 (s, CH C₅H₄), 72.03 (d, *J*_{PC} = 4 Hz, CH C₅H₄), 73.71 (d, *J*_{PC} = 15 Hz, CH C₅H₄), 76.03 (d, *J*_{PC} = 6 Hz, C^{ipso}-P C₅H₄), 84.86 (s, C^{ipso}-C C₅H₄), 120.50 (s, CH C₃H₂N₂), 126.79 (s, CH C₃H₂N₂), 128.14 (d, *J*_{PC} = 7 Hz, CH PPh₂), 128.49 (CH PPh₂), 133.52 (d, *J*_{PC} = 20 Hz, CH PPh₂), 139.19 (d, *J*_{PC} = 10 Hz, C^{ipso} PPh₂), 147.20 (s, C^{ipso} C₃H₂N₂). HRMS (ESI+), *m/z* calc. for C₂₇H₂₆FeN₂P ([**M** + H]⁺): 465.1177; found: 465.1172. Anal. Calc. for C₂₇H₂₅FeN₂P·0.1CH₂Cl₂ (472.8): C 68.84, H 5.37, N 5.92%. Found: C 68.77, H 5.24, N 6.02%.

Synthesis of [PdCl₂(1-κ²P,N)] (5). A 25 mL flask equipped with a magnetic stirring bar was charged with **1** (24.0 mg, 0.050 mmol) and [PdCl₂(MeCN)₂] (13.0 mg, 0.050 mmol). The solids were dissolved in anhydrous dry dichloromethane (5 mL), and the resulting red–orange solution was stirred for 30 min. Subsequent evaporation afforded complex **5** as an orange powder. Yield: 30.0 mg (quantitative). The crystal used for structure determination was grown from chloroform–hexane.

¹H NMR (400 MHz, CD₂Cl₂ + ca. 20% CD₃OD): δ 2.87 (br s, 1 H, C₅H₄), 3.80 (br s, 1 H, C₅H₄), 4.07 (s, 3 H, CH₃), 4.32–4.36 (m, 2 H, C₅H₄), 4.36–4.39 (m, 1 H, C₅H₄), 4.41–4.44 (m, 1 H, C₅H₄), 4.51–4.55 (m, 1 H, C₅H₄), 5.05–5.09 (m, 1 H, C₅H₄), 6.58 (d, *J* = 1.7 Hz, 1 H, C₃H₂N₂), 6.86 (d, *J* = 1.7 Hz, 1 H, C₃H₂N₂), 7.06 (s, 1 H, CHO), 7.38–7.49 (m, 4 H, PPh₂), 7.49–7.58 (m, 2 H, PPh₂), 7.58–7.69 (m, 2 H, PPh₂), 7.72–7.81 (m, 2 H, PPh₂). The CHO signal was not observed. ³¹P{¹H} NMR (162 MHz, CD₂Cl₂ and ca. 20% CD₃OD) δ 22.3 (s, PPh₂). ¹H NMR (400 MHz, dms_o-d₆): δ 2.70 (br s 1 H, C₅H₄), 3.60 (br s 1 H, C₅H₄), 4.00 (s, 3 H, CH₃), 4.34–4.38 (m, 2 H, C₅H₄), 4.45–4.49 (m, 1 H, C₅H₄), 4.49–4.53 (m, 1 H, C₅H₄), 4.60–4.65 (m, 1 H, C₅H₄), 5.05–5.09 (m, 1 H, C₅H₄), 6.47 (d, *J* = 1.7 Hz, 1 H, CHO), 6.54 (d, *J* = 4.1 Hz, 1 H, C₃H₂N₂), 6.90 (d, *J* = 4.1 Hz, 1 H, C₃H₂N₂), 7.20 (d, *J* = 1.7 Hz, 1 H, CHO), 7.41–7.63 (m, 8 H, PPh₂), 7.64–7.71 (m, 2 H, PPh₂). ³¹P{¹H} NMR (162 MHz, dms_o-d₆): δ 20.6 (s, PPh₂). ¹³C{¹H} NMR (100.6 MHz, CD₂Cl₂ + ca. 20% CD₃OD): δ 69.48 (s, CH C₅H₄), 69.71 (s, CHO), 70.56 (s, CH C₅H₄), 70.86 (s, CH C₅H₄), 72.47 (d, *J*_{PC} = 7 Hz, CH C₅H₄), 72.95 (d, *J*_{PC} = 11 Hz, CH C₅H₄), 74.75 (s, CH C₅H₄), 75.23 (d, *J*_{PC} = 8 Hz, CH C₅H₄), 76.68 (d, *J*_{PC} = 9 Hz, CH C₅H₄), 89.69 (s, C^{ipso}-C C₅H₄), 123.69 (s, CH C₃H₂N₂), ≈128.3 (s, CH C₃H₂N₂), 128.34 (d, *J*_{PC} = 12 Hz, CH PPh₂), 129.44 (d, *J*_{PC} = 12 Hz, CH PPh₂), ≈131.7 (d, *J*_{PC} = 3 Hz, CH PPh₂), 132.21 (d, *J*_{PC} = 3 Hz, CH PPh₂), 134.05 (d, *J*_{PC} = 11 Hz, CH PPh₂), 134.20 (d, *J*_{PC} = 11 Hz, CH PPh₂), ≈151 (s, C^{ipso} C₃H₂N₂). The ferrocene C^{ipso}-P signal was not observed. HRMS (ESI+), *m/z* calc. for C₂₇H₂₅ClFeN₂OPd ([**M** - Cl]⁺): 620.9771; found: 620.9776. Anal. Calc. for C₂₇H₂₅Cl₂FeN₂OPd·0.5CH₂Cl₂ (700.1): C 47.18, H 3.74, N 4.00%. Found: C 47.14, H 3.61, N 3.91%.

Synthesis of [Pd(1-κ²P,N)₂]Cl₂ (6a). A 25 mL flask equipped with a magnetic stirring bar was charged with **1** (24.0 mg, 0.05 mmol) and [PdCl₂(MeCN)₂] (6.5 mg, 0.025 mmol). Anhydrous dichloromethane (2 mL) was introduced, and the resulting red solution was stirred for 30 min. Evaporation produced complex **6a** as a dark orange solid. Yield: 28.5 mg (quantitative). The crystal used for structure determination was obtained from chloroform–hexane.

HRMS (ESI+), *m/z* calc. for C₅₄H₅₀Fe₂N₄O₂P₂Pd ([**M** - (Cl)₂]²⁺): 533.0566; found: 533.0562.

Synthesis of [Pd(1-κ²P,N)₂][BF₄]₂ (6b). A 25 mL flask was charged with **1** (19.2 mg, 0.040 mmol) and [Pd(MeCN)₄][BF₄]₂ (8.9 mg, 0.020 mmol). Anhydrous dichloromethane (4 mL) and anhydrous methanol (0.1 mL) were introduced successively, and the reaction mixture was stirred for 30 min. The resulting red solution was evaporated under vacuum, leaving **6b**·CH₂Cl₂ as a red solid. Yield: 26.6 mg (quantitative). Single crystals were obtained from a solution in dichloromethane–methanol overlaid with hexane.

³¹P{¹H} NMR (243.0 MHz, CD₃CN): δ 9.7 and 13.9 (2 × d, *J*_{PP} = 488 Hz, isomer A), 7.2 and 10.1 (2 × d, *J*_{PP} = 481 Hz, isomer B),

15.17 (s, isomer C), and 7.04 (s, isomer D).⁴⁵ HRMS (ESI+), *m/z* calc. for C₅₄H₅₀Fe₂N₄O₂P₂Pd ([M – 2BF₄]²⁺): 533.0566; found: 533.0534. Anal. Calc. for C₅₄H₅₀B₂F₈Fe₂N₄O₂P₂Pd·CH₂Cl₂ (1325.6): C 49.83, H 3.95, N 4.23%. Found: C 49.41, H 3.82, N 4.23%.

Preparation of [PdCl₂(2-κP)₂] (7). A 25 mL flask equipped with a magnetic stirring bar was charged with **3** (15.8 mg, 0.033 mmol) and [PdCl₂(MeCN)₂] (4.1 mg, 0.016 mmol). The solid educts were dissolved in anhydrous dichloromethane (2 mL), and the resulting solution was stirred for 30 min. Subsequent solvent removal under vacuum produced complex **7** as a red powder. Yield: 18.6 mg (quantitative). The crystal used for X-ray diffraction analysis was grown from chloroform–hexane.

¹H NMR (400 MHz, CDCl₃): δ 4.00 (s, 3 H, CH₃), 4.40 (vt, *J*' = 1.9 Hz, 2 H, C₅H₄), 4.62 (vt, *J*' = 1.9 Hz, 2 H, C₅H₄), 4.99 (vt, *J*' = 2.0 Hz, 2 H, C₅H₄), 5.57 (vt, *J*' = 2.0 Hz, 2 H, C₅H₄), 7.01 (d, *J* = 1.0 Hz, 1 H, C₃H₂N₂), 7.13 (d, *J* = 1.0 Hz, 1 H, C₃H₂N₂), 7.34–7.50 (m, 6 H, PPh₂), 7.61–7.69 (m, 4 H, PPh₂). ³¹P{¹H} NMR (162 MHz, CDCl₃): δ 14.7 (s, PPh₂). ¹³C{¹H} NMR (100.6 MHz, CDCl₃): δ 36.39 (s, CH₃), 72.97 (apparent t, *J* = 28 Hz, C^{ipso}-P C₅H₄), 73.57 (s, CH C₅H₄), 74.24 (apparent t, *J*_{PC} = 4 Hz, CH C₅H₄), 75.83 (s, CH C₅H₄), ≈ 76.7 (apparent t, CH C₅H₄; the signal is partly obscured by the solvent resonance), 79.37 (s, C^{ipso}-C C₅H₄), 126.20 (s, CH C₃H₂N₂), 127.84 (apparent t, *J* = 5 Hz, CH PPh₂), 128.93 (s, CH C₃H₂N₂), 130.38 (s, CH PPh₂), 130.87 (apparent t, *J* = 25 Hz, C^{ipso} PPh₂), 134.19 (apparent t, *J* = 6 Hz, CH PPh₂), 143.49 (s, C^{ipso} C₃H₂N₂), 186.99 (s, C=O). MS (ESI+), *m/z* 1097.1 ([M – Cl]⁺). Anal. Calc. for C₅₄H₄₆Cl₂Fe₂N₄O₂P₂Pd·CHCl₃ (1253.3): C 52.71, H 3.78, N 4.47%. Found: C 52.39, H 3.47, N 4.44%.

Synthesis of [PdCl₂(3-κ²P,N)₂] (8). A 25 mL flask equipped with a stirring bar was charged with **3**·0.2CH₂Cl₂ (26.7 mg, 0.055 mmol) and [PdCl₂(MeCN)₂] (14.4 mg, 0.055 mmol). Dry dichloromethane (2 mL) was added, and the orange solution was stirred for 30 min. Evaporation afforded complex **8** as an orange solid. Yield: 35.4 mg (quantitative). The crystal used for structure determination was obtained from chloroform.

¹H NMR (600.2 MHz, CD₂Cl₂): δ 2.52 (br s, 1 H, C₅H₄), 3.64 (d, *J* = 15.8 Hz, 1 H, CH₂), 3.66 (br s, 1 H, C₅H₄), 3.80 (s, 3 H, CH₃), 4.13 (br s, 1 H, C₅H₄), 4.22 (br s, 1 H, C₅H₄), 4.33 (br s, 1 H, C₅H₄), 4.35 (br s, 1 H, C₅H₄), 4.43 (br s, 1 H, C₅H₄), 4.80 (d, *J* = 15.8 Hz, 1 H, CH₂), 5.42 (br s, 1 H, C₅H₄), 6.45 (br s, 1 H, C₃H₂N₂), 6.78 (br s, 1 H, C₃H₂N₂), 7.38–7.44 (m, 2 H, PPh₂), 7.44–7.62 (m, 6 H, PPh₂), 7.79–7.86 (m, 2 H, PPh₂). ³¹P{¹H} NMR (243.0 MHz, CDCl₃) δ 22.3 (s, PPh₂). ¹³C{¹H} NMR (150.9 MHz, CD₂Cl₂): δ 25.51 (s, CH₂), 35.21 (s, CH₃), 68.97 (s, CH C₅H₄), 69.32 (s, CH C₅H₄), 69.59 (s, CH C₅H₄), 69.66 (d, *J*_{PC} = 61 Hz, C^{ipso}-P C₅H₄), 71.46 (d, *J*_{PC} = 7 Hz, CH C₅H₄), 73.02 (d, *J*_{PC} = 11 Hz, CH C₅H₄), 74.43 (d, *J*_{PC} = 8 Hz, CH C₅H₄), 76.06 (d, *J*_{PC} = 8 Hz, CH C₅H₄), 76.46 (s, CH C₅H₄), 88.12 (s C^{ipso}-C C₅H₄), 121.31 (s, CH C₃H₂N₂), 128.03 (d, *J*_{PC} = 11 Hz, CH PPh₂), 128.10 (s, CH C₃H₂N₂), 129.33 (d, *J*_{PC} = 11 Hz, CH PPh₂), ≈ 130 (2× C^{ipso} PPh₂), 131.27 (d, *J*_{PC} = 3 Hz, CH PPh₂), 131.93 (d, *J*_{PC} = 3 Hz, CH PPh₂), 133.93 (d, *J*_{PC} = 11 Hz, CH PPh₂), 134.17 (d, *J*_{PC} = 11 Hz, CH PPh₂), 152.05 (s, C^{ipso} C₃H₂N₂). HRMS (ESI+), *m/z* calc. for C₂₇H₂₅ClFeN₂PPd ([M – Cl]⁺): 604.9838; found: 604.9815. Anal. Calc. for C₂₇H₂₅Cl₂FeN₂PPd·1.5CH₂Cl₂ (769.0): C 44.51, H 3.67, N 3.64%. Found: C 44.97, H 3.21, N 3.70% (crystallised sample).

Preparation of [Pd(3-κ²P,N)₂][BF₄]₂ (9). Ligand **3** (27.9 mg, 0.060 mmol) and [Pd(MeCN)₄](BF₄)₂ (13.3 mg, 0.030 mmol) were mixed in acetonitrile (2 mL). The mixture was stirred for 30 min, and the resulting red–orange solution was evaporated under vacuum to produce complex **9** as an orange powder. Yield: 36.4 mg (quantitative).

Isomer A: ¹H NMR (400 MHz, CDCl₃): δ 3.45 (s, 3 H, CH₃), 3.61 (d, *J* = 16 Hz, 1 H, CH₂), 4.05 (d, *J* = 16 Hz, 1 H, CH₂), 4.25–4.27 (m, 1 H, C₅H₄), 4.32–4.35 (m, 1 H, C₅H₄), 4.36–4.39 (m, 1 H, C₅H₄), 4.46–4.49 (m, 1 H, C₅H₄), 4.55–4.59 (m, 1 H, C₅H₄), 4.62–4.65 (m, 1 H, C₅H₄), 4.94–4.97 (m, 1 H, C₅H₄), 5.08–5.12 (m, 1 H, C₅H₄), 6.87 (d, *J* = 2 Hz, 1 H, C₃H₂N₂), 6.93 (d, *J* = 2 Hz, 1 H, C₃H₂N₂). ³¹P{¹H} NMR (162 MHz, CDCl₃) δ 15.3 (s, PPh₂).

Isomer B: ¹H NMR (400 MHz, CDCl₃): δ 3.03 (s, 3 H, CH₃), 3.17–3.21 (m, 1 H, C₅H₄), 3.26 (d, *J* = 17 Hz, 1 H, CH₂), 3.83–3.85 (m, 1 H, C₅H₄), 4.24 (d, *J* = 17 Hz, 1 H, CH₂), 4.30–4.32 (m, 1 H, C₅H₄), 4.48–4.50 (m, 1 H, C₅H₄), 4.69–4.71 (m, 1 H, C₅H₄), 4.82–4.84 (m, 1 H, C₅H₄), 5.5 (very br s, C₅H₄), 6.1 (very br s, C₅H₄), 6.65 (d, *J* = 2 Hz, 1 H, C₃H₂N₂), 6.97 (d, *J* = 2 Hz, 1 H, C₃H₂N₂). ³¹P{¹H} NMR (162 MHz, CDCl₃) δ 12.5 (s, PPh₂).

Anal. Calc. for C₅₄H₅₀B₂F₈Fe₂N₄P₂Pd (1208.1): C 53.66, H 4.17, N 4.64%. Found: C 53.39, H 4.06, N 5.01%. Crystals suitable for structure determination were grown from dichloromethane–acetone.

Catalytic experiments. A Schlenk flask equipped with a magnetic stirring bar was charged successively with 4-tolylboronic acid (1.2 mmol), sodium carbonate (1.2 mmol), and the respective Pd catalyst (2 μmol, 0.2 mol.%). After three vacuum–nitrogen cycles, 2-bromopyridine (1.0 mmol) was added using an automatic pipette, and the flask was sealed with a rubber septum. Degassed benzene and degassed distilled water (2.0 mL each) were added, and the resulting mixture was heated at 50 °C under vigorous stirring for 6 h. After cooling to room temperature, anisole (1.0 mmol) was added as an internal standard. When the conversion efficiency was low, saturated aqueous sodium carbonate (3 mL) was added, and the mixture was shaken to dissolve the crystallised material. A small aliquot of the organic layer was removed, dried over MgSO₄, filtered through a PTFE syringe filter (pore size: 0.45 μm), and diluted with benzene-d₆. The yield was determined using ¹H NMR spectroscopy. The mercury poisoning test was performed similarly, with the mercury metal (≈50 mg) added before introducing the solvent.

Analytical data for 2-(4-methylphenyl)pyridine (**12**). ¹H NMR (400 MHz, CDCl₃): δ 2.40 (s, 3 H, CH₃), 7.18 (ddd, *J* = 6.2, 4.8, 2.3 Hz, 1 H, C₅H₄N), 7.26–7.31 (m, 2 H, C₆H₄), 7.65–7.76 (m, 2 H, C₅H₄N), 7.85–7.93 (m, 2 H, C₆H₄), 8.64–8.70 (m, 1 H, C₅H₄N). ¹³C{¹H} NMR (CDCl₃): δ 21.26 (s, CH₃), 120.24 (s, CH C₅H₄N), 121.78 (s, CH C₅H₄N), 126.77 (s, CH C₆H₄), 129.48 (s, CH C₆H₄), 136.60 (s, C^{ipso} C₆H₄), 136.67 (s, CH C₅H₄N), 138.94 (s, C^{ipso} C₆H₄), 149.58 (s, CH C₅H₄N), 157.46 (s, C^{ipso} C₅H₄N). The data match those in the literature.⁴⁶ HRMS (ESI+), *m/z* calc. for C₁₂H₁₂N ([M + H]⁺): 170.0970; found: 170.0958.

Conflicts of interest

There are no conflicts to declare.

Downloaded from www.rsc.org on 05/06/2016 09:39:45 AM. This article is licensed under a Creative Commons Attribution-NonCommercial 3.0 Unported Licence.



Data availability

The data supporting this article have been included as part of the supporting information (SI). Supporting information: a summary of the crystallographic parameters, additional structure diagrams, and copies of the NMR spectra. See DOI: <https://doi.org/10.1039/XXXX.CCDC2535619-2535625> contain the supplementary crystallographic data for this paper.

Acknowledgement

This work was supported by the Grant Agency of Charles University (project no. 235523) and the Charles University Research Centre program (project UNCE/24/SCI/010).

Notes and references

- 1 *Phosphorus(III) Ligands in Homogeneous Catalysis: Design and Synthesis*, eds. P. C. J. Kamer and P. W. N. M. van Leeuwen, Wiley: Chichester, 2012
- 2 (a) T. B. Rauchfuss in *Organometallic Coordination Chemistry and Catalysis*, ed. L. H. Pignolet, Springer, Boston, 1983, ch. 7, pp. 239-256; (b) A. Bader and E. Lindner, *Coord. Chem. Rev.*, 1991, **108**, 27; (c) C. S. Slone, D. A. Weinberger and C. A. Mirkin, *Progr. Inorg. Chem.*, 1999, **48**, 233; (d) P. Braunstein and F. Naud, *Angew. Chem. Int. Ed.*, 2001, **40**, 680.
- 3 W.-H. Zhang, S. W. Chien and T. S. A. Hor, *Coord. Chem. Rev.*, 2011, **255**, 1991.
- 4 V. Varmužová, I. Císařová and P. Štěpnička, *Dalton Trans.*, 2025, **54**, 16611.
- 5 (a) A. Togni, T. Hayashi, Eds., *Ferrocenes: Homogeneous Catalysis, Organic Synthesis, Materials Science*, VCH, Weinheim, 1995; (b) P. Štěpnička, Ed., *Ferrocenes: Ligands, Materials and Biomolecules*, Wiley, Chichester, 2008; (c) R. C. J. Atkinson, V. C. Gibson and N. J. Long, *Chem. Soc. Rev.*, 2004, **33**, 313; (d) R. Gómez Arrayás, J. Adrio and J. C. Carretero, *Angew. Chem. Int. Ed.*, 2006, **45**, 7674; (e) P. Štěpnička, *Dalton Trans.*, 2022, **51**, 8085.
- 6 For examples of similar "homologated" phosphinoferrrocene ligands, see: (a) P. Štěpnička, J. Schulz, T. Klemann, U. Siemeling and I. Císařová, *Organometallics*, 2010, **29**, 3187; (b) U. Siemeling, T. Klemann, C. Bruhn, J. Schulz and P. Štěpnička, *Dalton Trans.*, 2011, **40**, 4722; (c) U. Siemeling, T. Klemann, C. Bruhn, J. Schulz and P. Štěpnička, *Z. Anorg. Allg. Chem.*, 2011, **637**, 1824; (d) P. Štěpnička and I. Císařová, *Dalton Trans.*, 2013, **42**, 3373; (e) M. Zábanský, I. Císařová and P. Štěpnička, *Dalton Trans.*, 2015, **44**, 14494; (f) M. Zábanský, A. Machara, I. Císařová and P. Štěpnička, *Eur. J. Inorg. Chem.*, 2017, 4850; (g) O. Bárta, I. Císařová and P. Štěpnička, *Eur. J. Inorg. Chem.*, 2017, 489; (h) O. Bárta, I. Císařová, E. Mieczysławska, A. M. Trzeciak and P. Štěpnička, *Eur. J. Inorg. Chem.*, 2019, 4846; (i) M. Zábanský, I. Císařová and P. Štěpnička, *Eur. J. Inorg. Chem.*, 2017, 2557; (j) M. Zábanský and P. Štěpnička, *Eur. J. Inorg. Chem.*, 2025, e202500321.
- 7 (a) A. Labande, J.-C. Daran, E. Manoury and R. Poli, *Eur. J. Inorg. Chem.*, 2007, 1205; (b) S. Gülcemal, A. Labande, J.-C. Daran, B. Çetinkaya and R. Poli, *Eur. J. Inorg. Chem.*, 2009, 1806; (c) A. Labande, N. Debono, A. Sournia-Saquet, J.-C. Daran and R. Poli, *Dalton Trans.*, 2013, **42**, 6531.
- 8 I. R. Butler and R. L. Davies, *Synthesis*, 1996, 1350.
- 9 F. D. Popp and E. B. Moynahan, *J. Org. Chem.*, 1969, **34**, 454.
- 10 J. M. Brunel, B. Faure and M. Maffei, *Coord. Chem. Rev.*, 1998, **178-180**, 665.
- 11 For early examples of oxidations of ferrocenylmethanol using MnO₂, see: (a) J. K. Lindsay and C. R. Hauser, *J. Org. Chem.*, 1957, **22**, 355; (b) C. R. Hauser and J. K. Lindsay, *J. Org. Chem.*, 1957, **22**, 906.
- 12 H. Brisset, Y. Gourdel, P. Pellon and M. Le Corre, *Tetrahedron Lett.*, 1993, **34**, 4523.
- 13 The deprotection using 1 equiv. of dabco in THF overnight resulted in partial decomposition, thereby producing ketone **2** in a lower yield (32%). An improvement was observed when using an excess of dabco in anhydrous and degassed toluene at 50 °C for only 2 h (yield: 83%).
- 14 (a) D. N. Kursanov, Z. N. Parnes and N. M. Loim, *Synthesis*, 1974, 633; (b) T. Liu, X. Wang and D. Yin, *RSC Adv.*, 2015, **5**, 75794.
- 15 C. F. Nutaitis and B. D. Swartz, *Org. Prep. Proced. Int.*, 2005, **37**, 507.
- 16 Y. Kato and T. Mase, *Tetrahedron Lett.*, 1999, **40**, 8823 and ref. 33g.
- 17 X. Wu, A. K. Mahalingham and M. Alterman, *Tetrahedron Lett.*, 2005, **46**, 1501.
- 18 (a) D. Guillaneux and H. B. Kagan, *J. Org. Chem.*, 1995, **60**, 2502; (b) A. Muller, S. Otto and A. Roodt, *Dalton Trans.*, 2008, 650.
- 19 J. C. Green, *Chem. Soc. Rev.*, 1998, **27**, 263.
- 20 J. A. Adeleke and L.-K. Liu, *Acta Crystallogr., Sect. C: Cryst. Struct. Commun.*, 1993, **49**, 680.
- 21 Y. Zheng, J. A. Martinez-Acosta, M. Khimji, L. C. A. Barbosa, G. J. Clarkson and M. Wills, *ChemCatChem*, 2021, **13**, 4384.
- 22 (a) C. F. J. Barnard and M. J. H. Russell in *Comprehensive Coordination Chemistry: The Synthesis, Reactions, Properties and Applications of Coordination Compounds*, eds. G. Wilkinson, R. D. Gillard and J. A. McCleverty, Pergamon Press, Oxford, 1987, ch. 51, pp. 1099-1130; (b) A. T. Hutton and C. P. Morley in *Comprehensive Coordination Chemistry: The Synthesis, Reactions, Properties and Applications of Coordination Compounds*, eds. G. Wilkinson, R. D. Gillard and J. A. McCleverty, Pergamon Press, Oxford, 1987, ch. 51.9, pp. 1157-1170.
- 23 B. N. Storhoff and H. C. Lewis, Jr., *Coord. Chem. Rev.*, 1977, **23**, 1.
- 24 S. H. Strauss, *Chem. Rev.*, 1993, **93**, 927.
- 25 The palladium atom is displaced by 0.064(1) Å from the least-squares plane defined by the donor atoms {P1, N1, Cl1, C2}, which are coplanar within approximately 0.009 Å.
- 26 (a) B. Miller, J. Altman, C. Leschke, W. Schunack, K. Sünkel, J. Knizek, H. Noth and W. Beck, *Z. Anorg. Allg. Chem.*, 2000, 626, 978; (b) M. S. Szulmanowicz, W. Zawartka, A. Gniewek and A. M. Trzeciak, *Inorg. Chim. Acta*, 2010, **363**, 4346; (c) H. Sadaf, Imtiaz-ud-Din, S. S. Zahra, Ihsan-ul-Haq, S. Nadeem, M. N. Tahir, S. Ahmad and S. Andleeb, *Polyhedron*, 2019, **160**, 101.
- 27 (a) T. G. Appleton, H. C. Clark and L. E. Manzer, *Coord. Chem. Rev.*, 1973, **10**, 335; (b) F. R. Hartley, *Chem. Soc. Rev.*, 1973, **2**, 163.
- 28 R. G. Pearson, *Inorg. Chem.*, 1973, **12**, 712.
- 29 S. I. Kirin, H.-B. Kraatz and N. Metzler-Nolte, *Chem. Soc. Rev.*, 2006, **35**, 348.
- 30 P. Vosáhlo, J. Schulz, K. Škoch, I. Císařová and P. Štěpnička, *New J. Chem.*, 2019, **43**, 4463.



- 31 W. H. Hersh, *J. Chem. Educ.*, 1997, **74**, 1485.
- 32 M. Záborský, I. Císařová and P. Štěpnička, *Organometallics*, 2018, **37**, 1615.
- 33 Selected examples: (a) R. J. Coyle, Y. L. Slovokhotov, M. Y. Antipin and V. V. Grushin, *Polyhedron*, 1998, **17**, 3059; (b) P. Štěpnička, J. Podlaha, R. Gyepes and M. Poláček, *J. Organomet. Chem.*, 1998, **552**, 293; (c) V. C. Gibson, N. J. Long, A. J. P. White, C. K. Williams, D. J. Williams, M. Fontani and P. Zanello, *J. Chem. Soc., Dalton Trans.*, 2002, 3280; (d) P. Štěpnička, I. Císařová and R. Gyepes, *Eur. J. Inorg. Chem.*, 2006, 926; (e) J. Tauchman, I. Císařová and P. Štěpnička, *Organometallics*, 2009, **28**, 3288; (f) P. Štěpnička, H. Solařová, M. Lamač and I. Císařová, *J. Organomet. Chem.*, 2010, **695**, 2423; (g) P. Štěpnička, J. Schulz, T. Klemann, U. Siemeling and I. Císařová, *Organometallics*, 2010, **29**, 3187; (h) P. Štěpnička, H. Solařová and I. Císařová, *J. Organomet. Chem.*, 2011, **696**, 3727; (i) K. Škoch, I. Císařová, F. Uhlík and P. Štěpnička, *Dalton Trans.*, 2018, **47**, 16082; (j) F. Horký, I. Císařová, J. Schulz and P. Štěpnička, *J. Organomet. Chem.*, 2019, **891**, 44; (k) K. Škoch, P. Vosáhlo, I. Císařová and P. Štěpnička, *Dalton Trans.*, 2020, **49**, 1011; (l) V. Varmužová, F. Horký and P. Štěpnička, *New J. Chem.*, 2021, **45**, 3319; (m) O. Bárta, I. Císařová and P. Štěpnička, *Dalton Trans.*, 2021, **50**, 14662; (n) S. Dey, F. Roesler, C. Bruhn, Z. Kelemen and R. Pietschnig, *Inorg. Chem. Front.*, 2023, **10**, 3828 and refs. 6a, 6d and 6f-i.
- 34 (a) C. A. Hunter, K. R. Lawson, J. Perkins and C. J. Urch, *J. Chem. Soc., Perkin Trans. 2*, 2001, 651; (b) C. R. Martinez and B. L. Iverson, *Chem. Sci.*, 2012, **3**, 2191; (c) T. Chen, M. Li and J. Liu, *Cryst. Growth Des.*, 2018, **18**, 2765.
- 35 (a) N. Miyaura and A. Suzuki, *J. Chem. Soc., Chem. Commun.*, 1979, 866; (b) N. Miyaura, K. Yamada, and A. Suzuki, *Tetrahedron Lett.*, 1979, **20**, 3437.
- 36 (a) N. Miyaura and A. Suzuki, *Chem. Rev.*, 1995, **95**, 2457; (b) A. Suzuki, *J. Organomet. Chem.*, 1999, **576**, 147; (c) N. Miyaura, *Top. Curr. Chem.*, 2002, **219**, 11; (d) A. F. Littke and G. Fu, *Angew. Chem. Int. Ed.*, 2002, **41**, 4176; (e) N. Miyaura in *Metal-Catalyzed Cross-Coupling Reactions*, eds. A. De Meijere and F. Diederich, 2nd ed. Wiley-VCH, Weinheim, Germany, 2004, ch. 2, pp. 41-123; (f) I. P. Beletskaya, F. Alonso and V. Tyurin, *Coord. Chem. Rev.*, 2019, **385**, 137.
- 37 (a) X. A. F. Cook, A. de Gombert, J. McKnight, L. R. E. Pantaine and M. C. Willis, *Angew. Chem. Int. Ed.*, 2021, **60**, 11068; (b) E. A. Strømsodd, A. F. Buene, D. M. Almenningen, O. R. Gautun, and B. H. Hoff, *Dyes Pigm.*, 2023, **209**, 110899; (c) J. W. Meringdal and D. Menche, *Chem. Soc. Rev.*, 2025, **54**, 5746.
- 38 P. Štěpnička, I. Císařová and J. Schulz, *Organometallics*, 2011, **30**, 4393.
- 39 (a) N. T. S. Phan, M. Van Der Sluys and C. W. Jones, *Adv. Synth. Catal.*, 2006, **348**, 609; (b) M. C. D'Alterio, È. Casals-Cruaños, N. V. Tzouras, G. Talarico, S. P. Nolan and A. Poater, *Chem. Eur. J.*, 2021, **27**, 13481 and ref. 36.
- 40 (a) J. A. Widegren and R. G. Finke, *J. Mol. Catal. A: Chem.*, 2003, **198**, 317; (b) R. H. Crabtree, *Chem. Rev.*, 2012, **112**, 1536.
- 41 (a) D. F. Shriver and M. A. Drezdson, *The manipulation of air-sensitive compounds*, 2nd ed., Wiley: New York, 1986; (b) A. M. Borys, *Organometallics*, 2023, **42**, 182.
- 42 K. Škoch, I. Císařová, J. Schulz, U. Siemeling and P. Štěpnička, *Dalton Trans.*, 2017, **46**, 10339.
- 43 T. Hayashi, M. Konishi and M. Kumada, *Tetrahedron Lett.*, 1979, 1871.
- 44 R. M. Silverstein, F. X. Webster and D. J. Kiemle, *Spectrometric Identification of Organic Compounds*, 7th ed., Wiley, Hoboken, 2005.
- 45 The NMR data for isomers A and B were analysed as second-order spin systems using the online tool available at

http://anorganik.uni-tuebingen.de/klaus/nmr/spinsystems/index.php?p=ab_an (accessed on February 23, 2026). For a reference, see: H. Günther, *NMR Spectroscopy: Basic Principles, Concepts, and Applications in Chemistry*, 3rd ed., Wiley-VCH: Weinheim, 2013; ch. 6.4.4, p. 164 ff.

46 S. K. Gurung, S. Thapa, A. S. Vangala and R. Giri, *Org. Lett.*, 2013, **15**, 5378.

View Article Online
DOI: 10.1039/D6NJ01330A

Data availability statementView Article Online
DOI: 10.1039/D6NJ01330A

The data supporting this article have been included as part of the supporting information (SI). Supporting information: a summary of the crystallographic parameters, additional structure diagrams, and copies of the NMR spectra. See DOI: <https://doi.org/10.1039/XXXX>. CCDC 2535619-2535625 contain the supplementary crystallographic data for this paper.

1
2
3
4
5
6
7
8
9
10
11
12
13
14
15
16
17
18
19
20
21
22
23
24
25
26
27
28
29
30
31
32
33
34
35
36
37
38
39
40
41
42
43
44
45
46
47
48
49
50
51
52
53
54
55
56
57
58
59
60Downloaded on 05 June 2016 at 09:39:45 AM.
This article is licensed under a Creative Commons Attribution-NonCommercial 3.0 Unported Licence.
